# Covariant representations of the relativistic Brueckner T-matrix and the nuclear matter problem

T. Gross-Boelting, C. Fuchs and Amand Faessler

Institut für Theoretische Physik, Universität Tübingen, D-72076 Tübingen, Germany

#### Abstract

We investigate nuclear matter properties in the relativistic Brueckner approach. The in-medium on-shell T-matrix is represented covariantly by five Lorentz invariant amplitudes from which we deduce directly the nucleon self-energy. We discuss the ambiguities of this approach and the failure of previously used covariant representations in reproducing the nucleon self-energies on the Hartree-Fock level. To enforce correct Hartree-Fock results we develop a subtraction scheme which treats the bare nucleon-nucleon potential exactly in accordance to the different types of meson exchanges. For the remaining ladder kernel, which contains the higher order correlations, we employ then two different covariant representations in order to study the uncertainty inherent in the approach. The nuclear matter bulk properties are only slightly sensitive on the explicit representation used for the kernel. However, we obtain new Coester lines for the various Bonn potentials which are shifted towards the empirical region of saturation. In addition the nuclear equation-of-state turns out to be significantly softer in the new approach.

Key words: nuclear matter, relativistic Brueckner approach, self-energy PACS numbers: 21.30.+y, 21.65.+f, 24.10.Cn

#### 1 Introduction

The investigation of nuclear matter properties within the relativistic Dirac-Brueckner-Hartree-Fock (DBHF) approach [1–6] remains a fundamental topic in theoretical nuclear structure studies. Compared to non-relativistic approaches the relativistic DBHF treatment turned out to be a major step forward in the explanation of the saturation mechanism of nuclear matter. The saturation points obtained for non-relativistic calculations, throughout all possible choices of different nucleon-nucleon interactions, are located on the so called

'Coester line' [7] which does not meet the empirical saturation region. Using modern nucleon-nucleon interactions of the one-boson exchange type [8,9] the relativistic calculations also reveal such Coester lines which are, however, significantly shifted towards the empirical region [3].

On the other hand, many details of the relativistic theory are still not fully resolved. In particular, the precise form of the nucleon self-energy, i.e. the magnitude and the momentum dependence of the scalar and vector self-energy components are a question of current debate [3–5,10,11]. Since the self-energy describes the dressing of the particles inside the medium and thus determines the relativistic mean field this fact states a severe problem. Different techniques to handle the DBHF problem can lead to significantly different results [3–6,11]. In a recent work [5] we found that the momentum dependence of the nucleon self-energy is dominated by the one-pion exchange contribution which accounts for the nuclear tensor force.

Unfortunately, the treatment of the  $\pi NN$  vertex and the corresponding self-energy contributions is closely connected to a severe ambiguity in the T-matrix representation [5,10]. The DBHF approach starts from a realistic nucleon-nucleon potential of the one-boson exchange type, i.e. the Bonn potentials [12]. As for the free two-body scattering problem, anti-particle states are neglected, and thus one works exclusively with positive energy states. Hence, a direct determination of the nucleon self-energy operator is not possible since not all matrix elements of this operator are known. Horowitz and Serot have therefore developed a projection technique to determine the scalar and vector self-energy components from the in-medium T-matrix [1]. In this approach the T-matrix is represented covariantly by Dirac operators and Lorentz invariant amplitudes where the latter are determined from the positive-energy on-shell T-matrix elements.

The whole problem arises from the fact mentioned above, namely that one does not include negative energy states and therefore neglects the excitation of anti-nucleons. The inclusion of negative energy excitations with 4 states for each spinor yields  $4^4 = 256$  types of two-body matrix elements concerning their spinor structure. Symmetry arguments reduce this to 44 for on-shell particles. [13]. If one takes now only positive energy solutions into account this reduces to  $2^4 = 16$  two-body matrix elements. Considering in addition only on-shell matrix elements the number of independent matrix elements can be further reduced by symmetry arguments down to 5. Thus, all on-shell two-body matrix elements can be expanded into five Lorentz invariants. But these five invariants are not unique since the Dirac matrices involve always also negative energy states and thus a decomposition of the one-body nucleon-nucleon potential into a Lorentz scalar and a Lorentz vector contribution depends on the choice of these five Lorentz invariants mentioned above. The best choice would be to separate completely the negative energy Dirac states. But since this is not

possible, there is not a unique but only an 'optimal choice'. The topic of this paper is the form of this 'optimal choice' of the five invariants.

Thus, as discussed in [5], various covariant representations of the T-matrix exist which all reproduce identically the on-shell T-matrix elements but lead to rather different results for the nucleon self-energy in the present formalism. This ambiguity was found to arise substantially from the treatment of the pion exchange part, in particular by the way how to take the pseudo-vector nature of the  $\pi$ NN vertex into account. In realistic nucleon-nucleon potentials the pion is usually described by a pseudo-vector coupling [12]. A pseudo-vector  $\pi$ NN vertex is also predicted by the non-linear  $\sigma$ -model based on chiral symmetry [14]. Furthermore, a pseudo-vector  $\pi$ NN vertex has the advantage that it is consistent with neglection of negative energy states while a pseudo-scalar coupling connects very strongly positive and negative energy states.

Following this argumentation in several works [2,4,10,15] the so called 'pseudovector choice' to the T-matrix representation was applied. This means to simply replace the pseudo-scalar by a pseudo-vector covariant while keeping the corresponding amplitudes unchanged. However, this procedure is not well defined since equivalent ps representations exist which lead to non-equivalent pvrepresentations. A strong momentum dependence of the nucleon self-energy emerges, e.g., in the 'conventional' pv representation as it was applied by Sehn et al. [4]. In Ref. [5] we addressed the problem with the above ambiguity, in particular with respect to the determination of the nuclear self-energy components. There we also proposed a 'complete' pv representation of the T-matrix which results in a much weaker momentum dependence of the nucleon selfenergy as found in [4]. The latter representation is not only more consistent with the approximation scheme of the current DBHF approach but also works correctly at the Hartree-Fock level using the pseudo-vector pion exchange. This minimal requirement, namely that the complete procedure is able to reproduce the correct Hartree-Fock results, was never verified for other representations and indeed, the 'conventional' pv representation fails in this respect. Hence, a strong momentum dependence observed for the nucleon self-energy [4] appears to be the artifact of a misrepresentation of the pion exchange potential in the previously used 'conventional' pv representations [2,4,15].

In this paper we want to go beyond the investigation of Ref. [5]. There we tried to determine the range of uncertainty inherent in the present Brueckner approach by the consideration of the two limiting cases, namely the pseudo-scalar and the complete pseudo-vector representation of the T-matrix. One has, however, some additional 'leading order' information on the Lorentz structure of the T-matrix, which is given by the Born part, i.e. the bare nucleon-nucleon potential. If we want to reproduce the analytically known Hartree-Fock results [16] for the complete set of the six non-strange mesons used in the Bonn potential, only a mixed 'ps + pv' representation can be successful where the

different parts of the bare potential are represented separately either as ps or pv. It is clear that such a mixed representation is not feasible at the DBHF level since we can not disentangle the different meson contributions from the full in-medium interaction. To proceed, however, we suggest a subtraction method to the in-medium T-matrix which means to subtract the bare interaction, i.e. the leading order, from the full T-matrix and to treat the bare part the Hartree-Fock level - in the mixed ps + pv representation. The remaining ladder kernel or 'subtracted T-matrix', as we will call it in the following, i.e. the sum of all higher order exchange graphs, is then represented in different ways, either as pure ps or 'complete' pv. Applying these two representation schemes we are now able to reduce the range of uncertainty concerning the T-matrix representation to a minimum. The remaining uncertainty is inherent in the current DBHF approach and can not be removed by standard methods. The deviations in the final results are, however, small and – similar to the treatment of Ref. [5] – the momentum dependence of the self-energy is found to be rather weak. Furthermore we obtain new 'Coester lines' for Bonn A, B, C with, compared to previous works [3,4], improved saturation properties. Most remarkably is a strong softening of the nuclear equation-of-states.

The paper is now organized as follows: In section 2 we briefly review the Dirac-Brueckner Hartree-Fock approach and present some details on the calculation of the in-medium on-shell T-matrix elements. In section 3 we introduce the projection technique and discuss the different covariant representations used for the on-shell T-matrix. The subtraction method is developed at the end of this section. The nucleon self-energy in the medium and the nuclear matter bulk properties are then presented elaborately in section 4. At the end we summarize and conclude our work.

#### 2 The relativistic Brueckner approach

#### 2.1 The coupled set of equations

In the relativistic Brueckner approach the nucleon inside the nuclear medium is viewed as a dressed particle in consequence of its two-body interaction with the surrounding nucleons. The in-medium interaction of the nucleons is treated in the ladder approximation of the relativistic Bethe-Salpeter equation

$$T = V + i \int VQGGT \quad , \tag{1}$$

where T denotes the T-matrix. V is the bare nucleon-nucleon interaction. The intermediate off-shell nucleons in the scattering equation are described by a

two-particle propagator iGG. As usually done, we replace this propagator by an effective propagator [17], here the Thompson propagator [18] which allows only positive energy nucleons in the intermediate scattering states. In addition this propagator fixes also the off-shell behavior of the nucleons. This reduces the four-dimensional Bethe-Salpeter equation to a three-dimensional integral equation. The Pauli operator Q in the Thompson equation accounts for the influence of the medium by the Pauli-principle and projects the intermediate scattering states out of the Fermi sea.

The Green's function G which describes the propagation of dressed nucleons in the medium fulfills the Dyson equation

$$G = G_0 + G_0 \Sigma G \quad . \tag{2}$$

 $G_0$  denotes the free nucleon propagator while the influence of the surrounding nucleons is expressed by the nucleon self-energy  $\Sigma$ . In Brueckner theory this self-energy is determined by summing up the interaction with all the nucleons inside the Fermi sea

$$\Sigma = -i \int_{F} (Tr[GT] - GT) \quad . \tag{3}$$

The Hartree-Fock form of the self-energy integral is necessary if we use an 'unphysical' T-matrix, as done in [1]. However, since we will entirely work with anti-symmetrized two-nucleon states, our T-matrix is 'physical' and contains implicitly 'direct' and 'exchange' contributions. Hence, the Hartree form

$$\Sigma = -i \int_{F} Tr[GT] \tag{4}$$

of the self-energy integral is sufficient in our case. We will come back to this point in more detail in section 3. Since the three equations (1), (2) and (4) are strongly coupled, one has to solve this set of equations self-consistently.

The Dirac structure of the self-energy in isospin saturated nuclear matter follows from translational and rotational invariance, parity conservation and time reversal invariance [19]. In the nuclear matter rest frame the self-energy has the simple form

$$\Sigma(k, k_{\rm F}) = \Sigma_{\rm s}(k, k_{\rm F}) - \gamma_0 \,\Sigma_{\rm o}(k, k_{\rm F}) + \boldsymbol{\gamma} \cdot \mathbf{k} \,\Sigma_{\rm v}(k, k_{\rm F}) \quad , \tag{5}$$

with  $k_{\mu}$  being the nucleon four-momentum. The self-energy components depend as Lorentz scalar functions on the Lorentz invariants  $k^2$ ,  $k \cdot j$  and  $j^2$ ,

where  $j_{\mu}$  denotes the baryon current. In the nuclear matter rest frame this current is identical to  $j_{\mu} = \rho \delta_{\mu 0}$ , with  $\rho$  being the nuclear matter density. Hence, the Lorentz invariants can be expressed in terms of  $k_0$ ,  $|\mathbf{k}|$  and  $k_{\rm F}$ , where  $k_{\rm F}$  denotes the Fermi momentum, related to the density via  $\rho = 2k_{\rm F}^3/(3\pi^2)$ . By taking the traces in Dirac space as [1,4]

$$\Sigma_{\rm s} = \frac{1}{4} tr \left[ \Sigma \right] \quad , \quad \Sigma_{\rm o} = \frac{-1}{4} tr \left[ \gamma_0 \Sigma \right] \quad , \quad \Sigma_{\rm v} = \frac{-1}{4 |\mathbf{k}|^2} tr \left[ \boldsymbol{\gamma} \cdot \mathbf{k} \Sigma \right] \quad (6)$$

one can calculate the different Lorentz components of the self-energy from the self-energy operator (4).

The presence of the medium leads to effective masses and effective momenta

$$m^*(k, k_{\rm F}) = M + Re\Sigma_{\rm s}(k, k_{\rm F})$$
 ,  $k_{\mu}^* = k_{\mu} + Re\Sigma_{\mu}(k, k_{\rm F})$  (7)

of the nucleons. Above the Fermi surface the self-energy is generally complex due to possible decay of particle states into hole states within the Fermi sea. To simplify the self-consistency scheme we neglect this decay process and work in the so called 'quasi-particle approximation'. Since we only deal with the real part of the self-energy we omit this in the notation from now on.

Defining reduced effective quantities [4,5]

$$\tilde{k}_{\mu}^* = k_{\mu}^* / (1 + \Sigma_{\rm v}(k, k_{\rm F})) , \, \tilde{m}^*(k, k_{\rm F}) = m^*(k, k_{\rm F}) / (1 + \Sigma_{\rm v}(k, k_{\rm F})) , \, (8)$$

the Dirac equation in the nuclear matter rest frame can be rewritten as

$$[\gamma_{\mu}\tilde{k}^{*\mu} - \tilde{m}^{*}(k, k_{\rm F})]u(k, k_{\rm F}) = 0$$
(9)

which resembles a quasi-free Dirac equation for dressed nucleons. In general the reduced effective mass is density but also momentum dependent. To simplify the calculation, however, we fix the effective mass of the nucleon in the nuclear matter rest frame at the reference momentum  $|\mathbf{k}| = k_F$ . In this 'reference spectrum approximation' [20] the reduced effective mass  $\tilde{m}_F^* = \tilde{m}^*(|\mathbf{k}| = k_F)$  works as a self-consistency parameter in the current DBHF approach. All equations are iterated until  $\tilde{m}_F^*$  is converged to a fixed value. The 'reference spectrum approximation' implies that the self-energy itself is rather weakly momentum dependent. At the end of the calculation one has to verify the consistency of the assumption  $\Sigma(k) \approx \Sigma(|\mathbf{k}| = k_F)$  with the outcome of the iteration procedure.

Utilizing the different approximations discussed above the positive-energy inmedium nucleon spinor are given as

$$u_{\lambda}(k, k_{\rm F}) = \sqrt{\frac{\tilde{E}^*(\mathbf{k}) + \tilde{m}_F^*}{2\tilde{m}_F^*}} \begin{pmatrix} 1\\ \frac{2\lambda|\mathbf{k}|}{\tilde{E}^*(\mathbf{k}) + \tilde{m}_F^*} \end{pmatrix} \chi_{\lambda} , \qquad (10)$$

where  $\tilde{E}^*(\mathbf{k}) = \sqrt{\mathbf{k}^2 + \tilde{m}_F^{*2}}$ .  $\chi_{\lambda}$  above denotes a two-component Pauli spinor with  $\lambda = \pm \frac{1}{2}$  and the normalization of the Dirac spinor is  $\bar{u}_{\lambda}(k, k_{\mathrm{F}})u_{\lambda}(k, k_{\mathrm{F}}) = 1$ . Since the in-medium nucleon spinor contains the reduced effective mass the matrix elements of the bare nucleon-nucleon interaction are density dependent. This density effect does not appear in non-relativistic Brueckner calculations. It is believed that it is the main reason for the success of the DBHF approach in describing the saturation of nuclear matter [21].

#### 2.2 The in-medium T-matrix

We apply the relativistic Thompson equation [18] to solve the scattering problem of two nucleons in the nuclear medium. In the two-particle center of mass (c.m.) frame - the natural frame for studying the two-particle scattering process - this Thompson equation can be written as [2,4]

$$T(\mathbf{p}, \mathbf{q}, x)|_{c.m.} = V(\mathbf{p}, \mathbf{q})$$

$$+ \int \frac{d^3 \mathbf{k}}{(2\pi)^3} V(\mathbf{p}, \mathbf{k}) \frac{\tilde{m}_F^{*2}}{\tilde{E}^{*2}(\mathbf{k})} \frac{Q(\mathbf{k}, x)}{2\tilde{E}^{*}(\mathbf{q}) - 2\tilde{E}^{*}(\mathbf{k}) + i\epsilon} T(\mathbf{k}, \mathbf{q}, x) ,$$
(11)

where  $\mathbf{q} = (\mathbf{q}_1 - \mathbf{q}_2)/2$  is the relative three-momentum of the initial state while  $\mathbf{k}$  and  $\mathbf{p}$  are the relative three-momenta of the intermediate and final states, respectively. The total four-momentum of the two-nucleon system is  $\tilde{P}^* = \tilde{q}_1^* + \tilde{q}_2^*$ , which in the c.m. frame becomes  $\tilde{P}^* = (\tilde{P}_0^*, \mathbf{0})$ .  $\tilde{P}_0^* = \sqrt{\tilde{s}^*} = 2\tilde{E}^*(\mathbf{q}) = 2\sqrt{\mathbf{q}^2 + \tilde{m}_F^{*2}}$  is the starting energy in (11). If  $\mathbf{q}_1$  and  $\mathbf{q}_2$  are nuclear matter rest frame momenta of the nucleons in the initial state, the boost-velocity  $\mathbf{u}$  into the c.m. frame is given by

$$\mathbf{u} = \mathbf{P} / \sqrt{\tilde{s}^* + \mathbf{P}^2} \quad , \tag{12}$$

with the total three-momentum and the invariant mass  $\mathbf{P} = \mathbf{q}_1 + \mathbf{q}_2$  and  $\tilde{s}^* = (\tilde{E}^*(\mathbf{q}_1) + \tilde{E}^*(\mathbf{q}_2))^2 - \mathbf{P}^2$ , respectively. In Eq. (12) x denotes the set of additional parameters  $x = \{k_F, \tilde{m}_F^*, |\mathbf{u}|\}$  on which the T-matrix depends.

Applying standard techniques as explained in detail by Erkelenz [8] we solve the Thompson equation in the c.m. frame and calculate the plane-wave helicity matrix elements of the T-matrix. To determine the self-energy only positiveenergy T-matrix elements at on-shell points  $|\mathbf{p}| = |\mathbf{q}|$  are necessary since in (4) we use instead of the full nucleon propagator the Dirac propagator [1,19]

$$G^{D}(q) = [\gamma_{\mu}\tilde{q}^{*\mu} + \tilde{m}_{F}^{*}]2\pi i\delta(\tilde{q}^{*2} - \tilde{m}_{F}^{*2})\Theta(\tilde{q}_{0}^{*})\Theta(k_{F} - |\mathbf{q}|) \quad . \tag{13}$$

Here q denotes the nuclear matter rest frame momentum of the nucleon in the Fermi sea. This momentum is on-mass shell, therefore only elastic scattering amplitudes, i.e. on-shell T-matrix elements, contribute to the nucleon self-energy. Due to the  $\Theta$ -functions in the propagator only positive energy nucleons are allowed in the intermediate scattering state. Hence the subspace of negative energy states is omitted in the current Brueckner approach. In this way we avoid the delicate problem of infinities in the theory which would generally appear if we would include contributions from negative energy nucleons in the Dirac sea [1,6,22].

In the on-shell case parity and spin conservation demand that only five of sixteen possible positive-energy helicity matrix elements are linearly independent [17]. The five matrix elements are determined explicitly via the |JMLS| scheme. After a partial-wave projection onto the |JMLS| states, the Thompson equation reduces to a partially decoupled set of one-dimensional integral equations over the relative momentum  $|\mathbf{k}|$ . To accomplish such a reduction an angle-averaged Pauli-operator  $\overline{Q}$  is used instead of the full Pauli-operator Q. Since the Fermi sphere is deformed to a Fermi ellipsoid in the two-nucleon c.m. frame,  $\overline{Q}$  has to be evaluated for such a Fermi ellipsoid. The explicit expression for  $\overline{Q}$  can be found in Refs. [2,4,23]. Finally, the integral equations are solved numerically by the matrix inversion technique of Haftel and Tabakin [24].

Since the two-nucleon states are two-fermion states, we actually have to evaluate the fully anti-symmetrized matrix elements. Only these matrix elements are physically meaningful. Anti-symmetrization is achieved by restoring the total isospin of the two-nucleon system (I=0,1) with the help of the standard selection rule

$$(-1)^{L+S+I} = -1 . (14)$$

The five on-shell plane-wave helicity matrix elements for definite isospin are finally calculated from the five partial-wave helicity matrix elements obtained in the |JMLS> scheme by summing over the total angular momentum J as

$$\langle \mathbf{p}\lambda_{1}^{'}\lambda_{2}^{'}|T^{\mathrm{I}}(x)|\mathbf{q}\lambda_{1}\lambda_{2}\rangle = \sum_{\mathrm{J}} \left(\frac{2\mathrm{J}+1}{4\pi}\right) d_{\lambda^{'}\lambda}^{J}(\theta) \langle \mathbf{p}\lambda_{1}^{'}\lambda_{2}^{'}|T^{\mathrm{J},\mathrm{I}}(x)|\mathbf{q}\lambda_{1}\lambda_{2}\rangle. \tag{15}$$

 $\theta$  is the scattering angle between  $\mathbf{q}$  and  $\mathbf{p}$ , with  $|\mathbf{p}| = |\mathbf{q}|$ , while  $\lambda = \lambda_1 - \lambda_2$  and  $\lambda' = \lambda'_1 - \lambda'_2$ . The reduced rotation matrices  $d_{\lambda'\lambda}^{\mathbf{J}}(\theta)$  are those of Rose [25].

## 3 Covariant representations and the nucleon self-energy

## 3.1 Pseudo-scalar representation

To use the trace formulas, Eqs. (6), for the calculation of the nucleon selfenergy components one has to represent the T-matrix in the nuclear matter rest frame. Since we determine the T-matrix elements in the two-particle c.m. frame a representation with covariant operators and Lorentz invariant amplitudes in Dirac space is the most convenient way to Lorentz-transform the T-matrix from one frame into another [1]. A set of five linearly independent covariants is sufficient for such a T-matrix representation because on-shell only five helicity matrix elements appear as solution of the Thompson equation. A linearly independent although not unique set of five covariants is given by the Fermi covariants

$$S = 1 \otimes 1, V = \gamma^{\mu} \otimes \gamma_{\mu}, T = \sigma^{\mu\nu} \otimes \sigma_{\mu\nu}, A = \gamma_{5} \gamma^{\mu} \otimes \gamma_{5} \gamma_{\mu}, P = \gamma_{5} \otimes \gamma_{5}.$$
 (16)

Using this special set - the so called 'pseudo-scalar choice' - the on-shell T-matrix for definite isospin I can be represented covariantly as [1]

$$T^{\mathrm{I}}(|\mathbf{p}|, \theta, x) = F_{\mathrm{S}}^{\mathrm{I}}(|\mathbf{p}|, \theta, x) + F_{\mathrm{V}}^{\mathrm{I}}(|\mathbf{p}|, \theta, x) + F_{\mathrm{T}}^{\mathrm{I}}(|\mathbf{p}|, \theta, x) + F_{$$

Here  $\mathbf{p}$  and  $\theta$  denote the relative three-momentum and the scattering angle between the scattered nucleons in the c.m. frame, respectively. In addition, the five Lorentz invariant amplitudes  $F_i^{\mathrm{I}}(|\mathbf{p}|, \theta, x)$  with  $i = \{S, V, T, A, P\}$  depend also on  $x = \{k_{\mathrm{F}}, \tilde{m}_F^*, |\mathbf{u}|\}$ . We want to stress that the dependence of the amplitudes on  $|\mathbf{p}|$ ,  $\theta$  and x can be re-expressed in terms of Lorentz scalar quantities as explained in detail in [1]. Hence, the representation (17) is indeed fully covariant, only the calculation of the Lorentz invariant amplitudes is most easily performed in the two-particle c.m. frame.

We determine the Lorentz invariant amplitudes  $F_i^{\text{I}}(|\mathbf{p}|, \theta, x)$  by taking planewave helicity matrix elements of (17) in the c.m. frame. Using as abbreviation for the Fermi covariants the operators  $\Gamma_i$ , with  $\Gamma_i = \{S, V, T, A, P\}$ , the onshell matrix elements  $(|\mathbf{p}| = |\mathbf{q}|)$ , i.e. the solution of Eq. (15), and the invariant amplitudes are related by

$$<\mathbf{p}\lambda_{1}'\lambda_{2}'|T^{\mathrm{I}}(x)|\mathbf{q}\lambda_{1}\lambda_{2}> = \sum_{i} <\mathbf{p}\lambda_{1}'\lambda_{2}'|\Gamma_{i}|\mathbf{q}\lambda_{1}\lambda_{2}> F_{i}^{\mathrm{I}}(|\mathbf{p}|,\theta,x)$$
 (18)

Since the Fermi covariants are linearly independent, equation (18) can be inverted to determine the unknown amplitudes  $F_i^{\rm I}$ . The details of this inversion, especially the treatment of the kinematical singularities at  $\theta = 0$  and  $\theta = \pi$ , which appear likewise in the matrix elements  $d_{\lambda'\lambda}^{\rm J}(\theta)$ , Eq. (15) and  $\langle \mathbf{p}\lambda'_1\lambda'_2|\Gamma_i|\mathbf{q}\lambda_1\lambda_2 \rangle$ , are explained in [1,26].

Using physical plane-wave helicity matrix elements in (18) the Lorentz invariant amplitudes  $F_i^{\rm I}(|\mathbf{p}|, \theta, x)$  fulfill a specific anti-symmetry relation which is given by the Fierz transformation

$$F_i^{\mathbf{I}}(|\mathbf{p}|, \pi - \theta, x) = (-1)^{\mathbf{I}} F_i^{\mathbf{I}}(|\mathbf{p}|, \theta, x) \mathcal{F}_{ji} \quad , \tag{19}$$

where the Fierz matrix  $\mathcal{F}$  is the matrix given in Eq. (28). Due to this antisymmetry relation the 'direct' representation (17) for the T-matrix is sufficient and one can calculate the nucleon self-energy via the Hartree integral (4). Using explicitly momenta and Dirac indices, the self-energy reads

$$\Sigma_{\alpha\beta}(k, k_{\rm F}) = -i \int \frac{d^4q}{(2\pi)^4} G_{\tau\sigma}^D(q) T(|\mathbf{p}|, 0, x)_{\alpha\sigma, \beta\tau} \quad . \tag{20}$$

Here k and q denote the incoming and outgoing momenta of the two elastically scattered nucleons in the nuclear matter rest frame. The total energy of the two nucleons is  $\tilde{s}^* = (\tilde{E}^*(\mathbf{k}) + \tilde{E}^*(\mathbf{q}))^2 - \mathbf{P}^2$  and the total three-momentum, which defines the boost (12) into the two-particle c.m. frame, is  $\mathbf{P} = \mathbf{k} + \mathbf{q}$ . The relative momentum in the c.m. frame for which we determine the T-matrix is given by  $|\mathbf{p}| = \sqrt{\tilde{s}^*/4 - \tilde{m}_F^{*2}}$ . Since we only calculate the Hartree integral, the scattering angle is fixed to  $\theta = 0$ .

Applying the covariant representation (17) for the on-shell T-matrix the nucleon self-energy in isospin saturated nuclear matter is evaluated to be [4]

$$\Sigma_{\alpha\beta}(k, k_{\rm F}) = \int \frac{d^3 \mathbf{q}}{(2\pi)^3} \frac{\theta(k_{\rm F} - |\mathbf{q}|)}{\tilde{E}^*(\mathbf{q})} \left[ \tilde{m}_F^* 1_{\alpha\beta} F_{\rm S} + \tilde{\mathcal{I}}_{\alpha\beta}^* F_{\rm V} \right] \quad , \tag{21}$$

where the isospin averaged amplitudes are defined as

$$F_i(|\mathbf{p}|, 0, x) := \frac{1}{2} \left[ F_i^{I=0}(|\mathbf{p}|, 0, x) + 3F_i^{I=1}(|\mathbf{p}|, 0, x) \right]$$
 (22)

In the self-energy integral (21) only the anti-symmetrized scalar and vector amplitudes  $F_S$  and  $F_V$  for scattering angle  $\theta = 0$  (Hartree) contribute. This is not true if we use 'unphysical' helicity matrix elements as done by Horowitz and Serot [1]. If we neglect the selection rule (14), we have to determine explicitly the Hartree and the Fock contribution to the self-energy via

$$\Sigma_{\alpha\beta}(k,k_{\rm F}) = -i \int \frac{d^4q}{(2\pi)^4} G_{\tau\sigma}^D(q) [T(|\mathbf{p}|,0,x)_{\alpha\sigma,\beta\tau} - T(|\mathbf{p}|,\pi,x)_{\alpha\sigma,\tau\beta}] \quad .(23)$$

An equivalent procedure is to use the Hartree form (20) but with a T-matrix representation which explicitly contains 'direct' and 'exchange' terms. This is done by calculating 'unphysical' Lorentz invariant amplitudes  $\bar{F}_i^{\rm I}$  for scattering angles  $\theta$  and  $\pi - \theta$ , using Eq. (18) with non-antisymmetrized plane-wave helicity matrix elements. Then one defines interchanged Fermi covariants as [26]

$$\tilde{S} = \tilde{S}S$$
 ,  $\tilde{V} = \tilde{S}V$  ,  $\tilde{T} = \tilde{S}T$  ,  $\tilde{A} = \tilde{S}A$  ,  $\tilde{P} = \tilde{S}P$  , (24)

where the operator  $\tilde{S}$ , being the interchange covariant of S, exchanges the Dirac indices of particle 1 and 2, i.e.  $\tilde{S}u(1)_{\sigma}u(2)_{\tau} = u(1)_{\tau}u(2)_{\sigma}$ . The on-shell T-matrix is finally decomposed to

$$T^{I}(|\mathbf{p}|, \theta, x) = T^{I,D}(|\mathbf{p}|, \theta, x) - T^{I,X}(|\mathbf{p}|, \theta, x) \quad , \tag{25}$$

where the 'direct' part of the T-matrix is defined as

$$T^{\mathrm{I},D}(|\mathbf{p}|,\theta,x) = \left[\bar{F}_{\mathrm{S}}^{\mathrm{I}}(|\mathbf{p}|,\theta,x)\mathrm{S} + \bar{F}_{\mathrm{V}}^{\mathrm{I}}(|\mathbf{p}|,\theta,x)\mathrm{V} + \bar{F}_{\mathrm{T}}^{\mathrm{I}}(|\mathbf{p}|,\theta,x)\mathrm{T} + \bar{F}_{\mathrm{A}}^{\mathrm{I}}(|\mathbf{p}|,\theta,x)\mathrm{A} + \bar{F}_{\mathrm{P}}^{\mathrm{I}}(|\mathbf{p}|,\theta,x)\mathrm{P}\right] , \qquad (26)$$

while the 'exchange' part is given as

$$T^{\mathrm{I},X}(|\mathbf{p}|,\theta,x) = (-1)^{\mathrm{I}+1} \left[ \bar{F}_{\mathrm{S}}^{\mathrm{I}}(|\mathbf{p}|,\pi-\theta,x)\tilde{\mathrm{S}} + \bar{F}_{\mathrm{V}}^{\mathrm{I}}(|\mathbf{p}|,\pi-\theta,x)\tilde{\mathrm{V}} + \bar{F}_{\mathrm{T}}^{\mathrm{I}}(|\mathbf{p}|,\pi-\theta,x)\tilde{\mathrm{T}} + \bar{F}_{\mathrm{A}}^{\mathrm{I}}(|\mathbf{p}|,\pi-\theta,x)\tilde{\mathrm{A}} + \bar{F}_{\mathrm{P}}^{\mathrm{I}}(|\mathbf{p}|,\pi-\theta,x)\tilde{\mathrm{P}} \right]. \tag{27}$$

Since the interchanged and original Fermi covariants are related by the Fierz transformation  $\mathcal{F}$  [26] via

$$\begin{pmatrix}
\tilde{S} \\
\tilde{V} \\
\tilde{T} \\
\tilde{A} \\
\tilde{P}
\end{pmatrix} = \frac{1}{4} \begin{pmatrix}
1 & 1 & \frac{1}{2} & -1 & 1 \\
4 & -2 & 0 & -2 & -4 \\
12 & 0 & -2 & 0 & 12 \\
-4 & -2 & 0 & -2 & 4 \\
1 & -1 & \frac{1}{2} & 1 & 1
\end{pmatrix} \begin{pmatrix}
S \\
V \\
T \\
A \\
P
\end{pmatrix} , (28)$$

the 'exchange' contribution of the T-matrix is identical to

$$T^{I,X}(|\mathbf{p}|, \theta, x) = (-1)^{I+1} \sum_{ij} \bar{F}_i^{I}(|\mathbf{p}|, \pi - \theta, x) \mathcal{F}_{ij} \Gamma_j \quad . \tag{29}$$

Above only the Fermi covariants  $\Gamma_i$  appear and one can rewrite the T-matrix representation (25) in terms of a 'direct' representation as in (17). The fully anti-symmetrized Lorentz invariant amplitudes are therefore related to the non-antisymmetrized amplitudes via the identity

$$F_i^{\mathrm{I}}((|\mathbf{p}|, \theta, x) = \bar{F}_i^{\mathrm{I}}((|\mathbf{p}|, \theta, x) - (-1)^{\mathrm{I}+1} \bar{F}_i^{\mathrm{I}}((|\mathbf{p}|, \pi - \theta, x) \mathcal{F}_{ji} \quad . \tag{30}$$

These anti-symmetrized amplitudes respect the relation (19) and are identical to the amplitudes which we obtain when we use 'physical' plane-wave helicity matrix elements in (18) from the beginning. Nevertheless when employing the T-matrix representation (25) with the non-antisymmetrized amplitudes one obtains for the self-energy the expression given in Ref. [1]

$$\Sigma_{\alpha\beta}(k, k_{\rm F}) = \int \frac{d^3\mathbf{q}}{(2\pi)^3} \frac{\theta(k_{\rm F} - |\mathbf{q}|)}{4\tilde{E}^*(\mathbf{q})} \left[ \tilde{\mathcal{A}}_{\alpha\beta}^* \left( 4\bar{F}_{\rm V}^D - \bar{F}_{\rm S}^X + 2\bar{F}_{\rm V}^X + 2\bar{F}_{\rm A}^X + \bar{F}_{\rm P}^X \right) + \tilde{m}_F^* \mathbf{1}_{\alpha\beta} \left( 4\bar{F}_{\rm S}^D - \bar{F}_{\rm S}^X - 4\bar{F}_{\rm V}^X - 12\bar{F}_{\rm T}^X + 4\bar{F}_{\rm A}^X - \bar{F}_{\rm P}^X \right) \right]$$
(31)

where the isospin-averaged non-antisymmetrized amplitudes are defined as

$$\bar{F}_{i}^{D} := \frac{1}{2} \left[ \bar{F}_{i}^{I=0}(|\mathbf{p}|, 0, x) + 3\bar{F}_{i}^{I=1}(|\mathbf{p}|, 0, x) \right]$$
$$\bar{F}_{i}^{X} := \frac{1}{2} \left[ -\bar{F}_{i}^{I=0}(|\mathbf{p}|, \pi, x) + 3\bar{F}_{i}^{I=1}(|\mathbf{p}|, \pi, x) \right]$$
(32)

Due to relation (30) the nucleon self-energy defined via the integrals (21) or (31) is, of course, identical.

In Fig. 1 we show the result of a self-consistent DBHF calculation for the nucleon self-energy in nuclear matter applying as representation for the on-shell T-matrix the ps representation (17). As bare interaction we have used

the Bonn A potential [12] and, for comparison, the  $\sigma$ - $\omega$  model potential [29] which was originally used by Horowitz and Serot [1]. The density is chosen to be the empirical saturation density of nuclear matter with a Fermi momentum of  $k_{\rm F} = 1.34 fm^{-1}$ . As already discussed in Ref. [4], we see a pronounced mo-

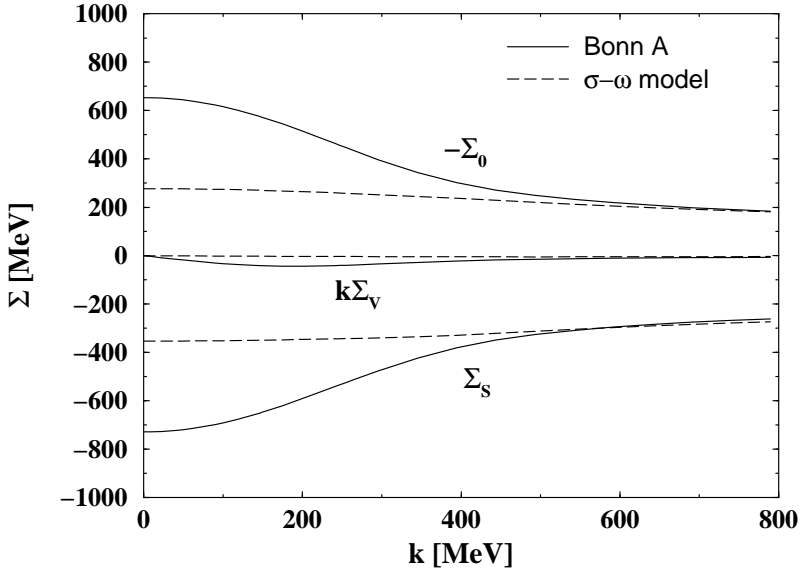


Fig. 1. Momentum dependence of the DBHF nucleon self-energy components in nuclear matter at  $k_{\rm F}=1.34fm^{-1}$  using as bare nucleon-nucleon potential Bonn A (solid) and the  $\sigma$ - $\omega$  model potential (dashed). For the T-matrix the ps representation (17) is applied.

mentum dependence of the nucleon self-energy components with the full Bonn A while in the case of the  $\sigma$ - $\omega$  model potential the dependence on the momentum is rather weak. A strong momentum dependence questions, of course, the validity of the 'reference spectrum approximation' used in the present self-consistency scheme. Furthermore, such a strong momentum dependence leads to unphysical results deep inside the Fermi sea since the effective mass drops to values which are close to zero. Therefore in Ref. [5] the strong momentum dependence of the self-energy was studied in more detail and found to originate mainly from the one-pion exchange contribution to the self-energy. To illustrate this aspect, in Fig. 2 the result of a non-selfconsistent Hartree-Fock (HF) calculation are shown. The HF nucleon self-energy is defined via the integral

$$\Sigma^{HF} = -i \int_{F} Tr[G^{D}V] \quad . \tag{33}$$

As in the case of the full DBHF calculation we determine at first the matrix elements of V and apply afterwards the ps representation (17) for the matrix elements. For better comparison to Fig. 1 we have fixed the Fermi momentum again at  $k_{\rm F} = 1.34 fm^{-1}$  while for the effective mass, necessary to calculate the propagator  $G^D$  and the dressed potential V, we have taken a fixed value of

 $\tilde{m}_F^* = 500 MeV$ . With the full Bonn potential the Hartree-Fock nucleon self-

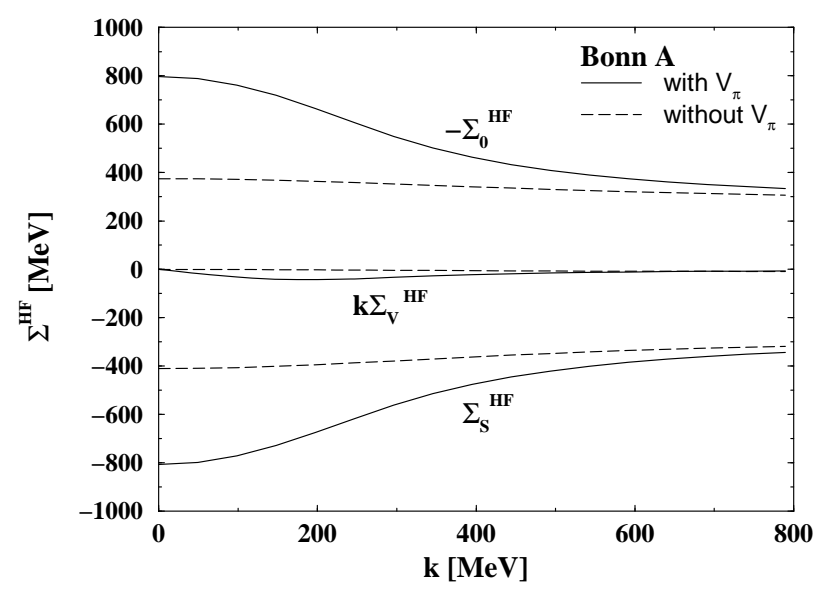


Fig. 2. Momentum dependence of the Hartree-Fock nucleon self-energy components in nuclear matter at  $k_{\rm F} = 1.34 fm^{-1}$ . The reduced effective mass of the nucleon is fixed at  $\tilde{m}_F^* = 500 MeV$ . As nucleon-nucleon interaction the Bonn A potential with (solid) and without (dashed) pion exchange part is used. For the bare interaction the ps representation (17) is applied.

energy is similar to the result of the self-consistent DBHF calculation. On the other hand applying Bonn A without the pion exchange part, the Hartree-Fock nucleon self-energy is weakly momentum dependent, as previously observed in the DBHF calculation with the  $\sigma$ - $\omega$  model potential. This shows that the pion exchange part within the Bonn potential is responsible for the strong momentum dependence in the nucleon self-energy. That the non-selfconsistent Hartree-Fock nucleon self-energy is also similar to the DBHF nucleon selfenergy in the case of the Bonn A potential indicates that the summation of the higher order ladder diagrams of the pion exchange has almost no effect on the form of the nucleon self-energy. It appears that the one-pion exchange dominates the whole momentum dependence in the nucleon self-energy. Although the HF and the DBHF self-energies are similar on the scale of some 100 MeV, one should, however, not conclude that the higher order correlations in the T-matrix are of minor importance. Since physical observables, like the single particle potential or the equation-of-state result from the cancellation of the large scalar and vector fields, they react extremely sensitive on small fluctuations on the scale of the self-energy. This is reflected, e.g., by the values of the binding energies per particle which is (at  $k_{\rm F} = 1.34 fm^{-1}$  for full Bonn A) E/A = -16.9 MeV for the DBHF and E/A = +19.3 MeV for the pure HF calculation. We will now consider the role of the pion in more detail.

## 3.2 Conventional pseudo-vector representation

The discussion of the pion-exchange contribution to the nucleon self-energy is intimately connected to an ambiguity of the T-matrix representation, as it was pointed out in [26]. The set of five covariants used to represent the on-shell T-matrix is not uniquely defined when one works exclusively in the subspace of positive energy states [22]. Obviously, various alternative sets of five linearly independent covariants exist which all can reproduce, like the Fermi covariants, the five on-shell helicity matrix elements of the T-matrix. For example, the pseudo-vector covariant

$$PV = \frac{\rlap/\bar{p}_1^* - \rlap/\bar{q}_1^*}{2\tilde{m}_F^*} \gamma_5 \otimes \frac{\rlap/\bar{p}_2^* - \rlap/\bar{q}_2^*}{2\tilde{m}_F^*} \gamma_5$$
 (34)

with  $\tilde{q}_i^*$  and  $\tilde{p}_i^*$  being the initial and final momenta of the nucleons, leads to identical on-shell helicity matrix elements as the pseudo-scalar covariant  $P = \gamma_5 \otimes \gamma_5$ . On-shell the nucleon spinors fulfill the quasi-free Dirac equation (9), with  $\tilde{m}_F^*$  fixed at a reference point, and therefore it holds

$$\bar{u}(p, k_{\rm F}) \frac{p^* - q^*}{2\tilde{m}_F^*} \gamma_5 u(q, k_{\rm F}) = \bar{u}(p, k_{\rm F}) \gamma_5 u(q, k_{\rm F}) \quad . \tag{35}$$

Thus, if we replace the pseudo-scalar covariant P in the T-matrix representation (17) by the pseudo-vector covariant PV and perform the inversion of Eq. (18), the calculated Lorentz invariant amplitude  $F_{\rm PV}$  will be identical to the previously calculated amplitude  $F_{\rm P}$ . Hence, the representation of the on-shell T-matrix is ambiguous in the detailed form of the covariant operators one can use which is crucial for the description of the one-pion exchange [5]. The  $\pi NN$  vertex in the OBE potentials, e.g. Bonn, is usually treated by a pseudo-vector coupling. In [27] in was shown that the  $\pi NN$  coupling is by less than 5% of pseudo-scalar nature at the on-shell point. There are several arguments which in addition strongly support a pseudo-vector vertex. First of all a PV vertex is consistent with soft pion theorems based on chiral symmetry considerations of QCD [14]. Secondly, the PV vertex suppresses the coupling to negative energy states due to the on-shell relation

$$\bar{v}(p, k_{\rm F}) \frac{\not p_1^* - \not q_1^*}{2\tilde{m}_F^*} \gamma_5 u(q, k_{\rm F}) = 0 \quad , \tag{36}$$

with  $v(p, k_{\rm F})$  a negative energy spinor. In [26] it was, e.g., shown that the onepion exchange contribution to the nuclear optical potential tends to increase drastically at low momenta if the  $\pi NN$  vertex is treated as pseudo-scalar. One reason for this behavior is the strong coupling to negative energy states which is not apparent in non-relativistic approaches. A pseudo-vector vertex is more consistent with the approximation scheme of the conventional Brueckner scheme where one neglects the negative energy states completely. It also strongly suppresses the pion contribution in particular at low energies which is more in accordance with the empirical knowledge from proton-nucleus scattering. One should expect therefore that in the DBHF approach a pseudo-vector coupling also drastically reduces the influence of the pion on the nucleon self-energy in the medium [1,2].

To account for the pseudo-vector nature of the pion exchange in the T-matrix, in the past the pseudo-scalar covariant P was simply replaced by the pseudo-vector covariant PV [2,4,28,10]. If one uses, however, the 'direct' ps representation of the T-matrix (17) and changes to a pv representation, the pseudo-vector amplitude  $F_{PV} = F_P$  will not contribute to the self-energy (21) since it does not appear in the Hartree integral. To suppress the pion contribution one needs to find a different pv representation of the T-matrix where the pseudo-vector covariant occurs in the Fock or 'exchange' part of the self-energy. One possible pv representation is given by the ps representation (25) with P and  $\tilde{P}$  replaced by PV and  $\tilde{P}$ V, respectively. The interchanged covariant  $\tilde{P}$ V is thereby defined as in [26] by applying the operator  $\tilde{S}$ , (24), to the covariant PV, (34), and by interchanging the final momenta  $\tilde{p}_1^*$  and  $\tilde{p}_2^*$  in Eq. (34). Performing this replacement the pseudo-vector amplitude  $\tilde{F}_{PV}^X = \tilde{F}_{P}^X$  contributes to the nucleon self-energy integral with a weight factor of [5]

$$Tr[(\tilde{A}^* + \tilde{m}_F^*)\widetilde{PV}] = -(\tilde{k}^* + \tilde{m}_F^*)(\frac{\tilde{k}_{\mu}^* \tilde{q}^{*\mu}}{2\tilde{m}_F^*} - \frac{1}{2})$$
 (37)

For comparison, with the ps representation (25) the weight factor of the pseudo-scalar amplitude  $\bar{F}_{\rm P}^X$  in the self-energy integral (31) is

$$Tr[(\tilde{p}^* + \tilde{m}_F^*)\tilde{P}] = -(\tilde{p}^* - \tilde{m}_F^*)$$
 (38)

Using the pv representation of the T-matrix as discussed above the nucleon self-energy becomes [2,4]

$$\Sigma_{\alpha\beta}(k, k_{\rm F}) = \int \frac{d^{3}\mathbf{q}}{(2\pi)^{3}} \frac{\Theta(k_{F} - |\mathbf{q}|)}{4\tilde{E}^{*}(\mathbf{q})} \left\{ (\tilde{k}_{\alpha\beta}^{*} - \tilde{\mathcal{A}}_{\alpha\beta}^{*}) \frac{2\tilde{q}_{\mu}^{*}(\tilde{k}^{*\mu} - \tilde{q}^{*\mu})}{4\tilde{m}_{F}^{*2}} \bar{F}_{PV}^{X} \right. \\
+ \tilde{m}_{F}^{*} 1_{\alpha\beta} \left[ 4\bar{F}_{S}^{D} - \bar{F}_{S}^{X} - 4\bar{F}_{V}^{X} - 12\bar{F}_{T}^{X} + 4\bar{F}_{A}^{X} - \frac{(\tilde{k}^{*\mu} - \tilde{q}^{*\mu})^{2}}{4\tilde{m}_{F}^{*2}} \bar{F}_{PV}^{X} \right] \\
+ \tilde{\mathcal{A}}_{\alpha\beta}^{*} \left[ 4\bar{F}_{V}^{D} - \bar{F}_{S}^{X} + 2\bar{F}_{V}^{X} + 2\bar{F}_{A}^{X} - \frac{(\tilde{k}^{*\mu} - \tilde{q}^{*\mu})^{2}}{4\tilde{m}_{F}^{*2}} \bar{F}_{PV}^{X} \right] \right\}. (39)$$

However, this self-energy appears to be unphysical since the amplitudes  $\bar{F}_i^{D,X}$  used in the integral are calculated from non-antisymmetrized helicity matrix elements of the T-matrix. It is by no means clear if the unphysical contributions do cancel as they do in the case when we use the ps representation of the T-matrix, i.e. see integrals (31) and (21). That the current pv representation

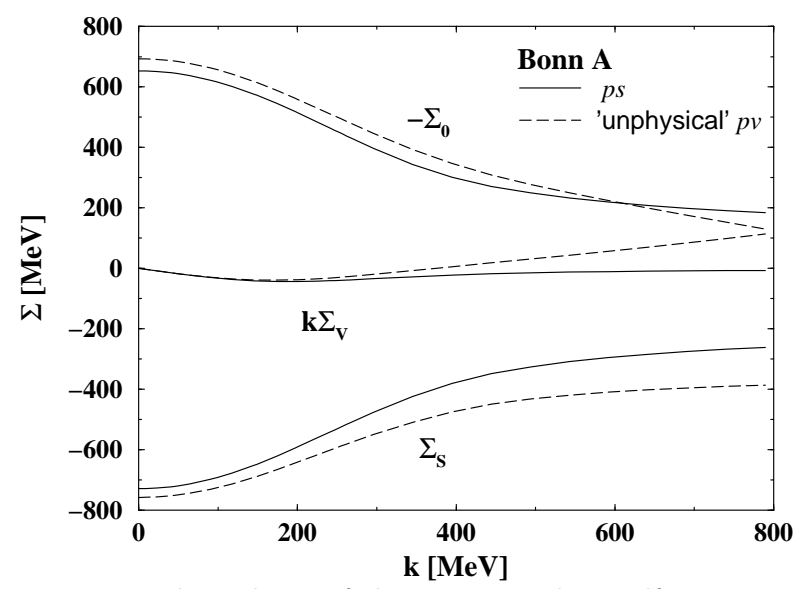


Fig. 3. Momentum dependence of the DBHF nucleon self-energy components in nuclear matter at  $k_{\rm F}=1.34fm^{-1}$  using the Bonn A potential. For the T-matrix the ps representation (Eq. (17), solid) and the 'unphysical' pv representation (as used in (39), dashed) are applied.

of the T-matrix is indeed unphysical can be seen in Fig. 3 where the nucleon self-energy components, evaluated from the integral (39), are shown. The self-energy components continue to be strongly momentum dependent. Furthermore, the vector component  $\Sigma_V$  shows an unphysical asymptotic behavior. Instead of dropping to zero its value increases with increasing momentum of the nucleon. This demonstrates that the pv representation of the T-matrix with non-antisymmetrized Lorentz invariant amplitudes  $\bar{F}_i^{\rm I}$ , as used in Eq. (39), is not useful.

To circumvent the problem of unphysical contribution to the nucleon selfenergy one should start from a different ps representation of the T-matrix where one uses anti-symmetrized amplitudes  $F_i^{\rm I}(|\mathbf{p}|, \theta, x)$  and  $F_i^{\rm I}(|\mathbf{p}|, \pi - \theta, x)$ instead of unphysical amplitudes  $\bar{F}_i^{\rm I}(|\mathbf{p}|, \theta, x)$  and  $\bar{F}_i^{\rm I}(|\mathbf{p}|, \pi - \theta, x)$ , respectively. One possible ps representation of the T-matrix is, for example, given by [4]

$$T^{\mathbf{I}}(|\mathbf{p}|, \theta, x) = T^{\mathbf{I}, D}(|\mathbf{p}|, \theta, x) - T^{\mathbf{I}, X}(|\mathbf{p}|, \theta, x) \quad . \tag{40}$$

where the 'direct' and 'exchange' parts of the T-matrix are defined as

$$T^{\mathrm{I},D}(|\mathbf{p}|,\theta,x) = \frac{1}{2} \left[ F_{\mathrm{S}}^{\mathrm{I}}(|\mathbf{p}|,\theta,x) \mathbf{S} + F_{\mathrm{V}}^{\mathrm{I}}(|\mathbf{p}|,\theta,x) \mathbf{V} + F_{\mathrm{T}}^{\mathrm{I}}(|\mathbf{p}|,\theta,x) \mathbf{T} + F_{\mathrm{A}}^{\mathrm{I}}(|\mathbf{p}|,\theta,x) \mathbf{A} + F_{\mathrm{P}}^{\mathrm{I}}(|\mathbf{p}|,\theta,x) \mathbf{P} \right] , \qquad (41)$$

and

$$T^{\mathrm{I},X}(|\mathbf{p}|,\theta,x) = (-1)^{\mathrm{I}+1} \frac{1}{2} \left[ F_{\mathrm{S}}^{\mathrm{I}}(|\mathbf{p}|,\pi-\theta,x)\tilde{\mathbf{S}} + F_{\mathrm{V}}^{\mathrm{I}}(|\mathbf{p}|,\pi-\theta,x)\tilde{\mathbf{V}} + F_{\mathrm{T}}^{\mathrm{I}}(|\mathbf{p}|,\pi-\theta,x)\tilde{\mathbf{T}} + F_{\mathrm{A}}^{\mathrm{I}}(|\mathbf{p}|,\pi-\theta,x)\tilde{\mathbf{A}} + F_{\mathrm{P}}^{\mathrm{I}}(|\mathbf{p}|,\pi-\theta,x)\tilde{\mathbf{P}} \right]. \tag{42}$$

Due to the anti-symmetry relation (19) for the Lorentz invariant amplitudes  $F_i^{\rm I}(|\mathbf{p}|, \theta, x)$  we have the identity

$$T^{I,X}(|\mathbf{p}|, \theta, x) = -T^{I,D}(|\mathbf{p}|, \theta, x) \tag{43}$$

and with the normalization factors  $\frac{1}{2}$  in (41) and (42) this leads to identical results for the self-energies as in the former cases, i.e. Eqs. (21) and (31).

If we replace now in (41) and (42) the covariants  $P, \tilde{P}$  by  $PV, \widetilde{PV}$ , respectively, we arrive at the 'conventional' pv representation as applied in Refs. [2,4,15]. The nucleon self-energy components calculated with this 'conventional' pv representation of the T-matrix are shown in Fig. 4. The behavior of the nucleon

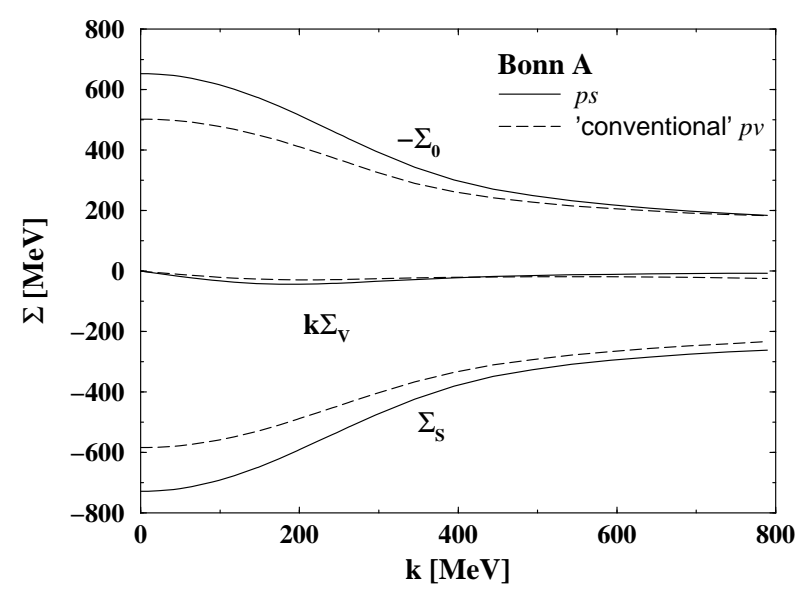


Fig. 4. Momentum dependence of the DBHF nucleon self-energy components in nuclear matter at  $k_{\rm F}=1.34fm^{-1}$  using the Bonn A potential. For the T-matrix the ps representation (Eq. (17), solid) and the 'conventional' pv representation (see text after Eq. (43), dashed) are applied.

self-energy components is similar to the case with the ps representation for the T-matrix, i.e. the momentum dependence is still pronounced, although

the absolute magnitude of the fields is reduced. As discussed in Ref. [5] this is due to the fact that the pion contribution is yet not correctly treated as pseudo-vector.

## 3.3 Complete pseudo-vector representation

To suppress the undesirable pseudo-scalar contribution of the pion to the nucleon self-energy we have to determine a different pv representation of the T-matrix. As starting point we should consider the Hartree-Fock level in more detail since the correct pv representation of the T-matrix should reproduce the HF nucleon self-energy when the pseudo-vector pion exchange potential is employed as bare nucleon-nucleon interaction. The 'conventional' pv representation discussed in the last section does not fulfill this minimal requirement. The reason is simply that due to the Fierz transformation (28) all Fermi covariants still contain pseudo-scalar contribution, i.e. the covariants (S,V,T,A,P) can be re-expressed in terms of  $(\tilde{S}, \tilde{V}, \tilde{T}, \tilde{A}, \tilde{P})$ . Hence, in the 'conventional' pv representation not all possible pseudo-scalar contributions are replaced by a pseudo-vector contribution when one simply replaces  $\tilde{P}$  with  $\tilde{PV}$  in Eq. (42). To obtain a 'complete' pv representation the identities

$$\frac{1}{2}(T + \tilde{T}) = S + \tilde{S} + P + \tilde{P}$$

$$\tag{44}$$

$$V + \tilde{V} = S + \tilde{S} - P - \tilde{P} \tag{45}$$

are actually very helpful. Since Tjon and Wallace already addressed this point in Ref. [26] we will follow now partially their notation. To obtain the 'complete' pv representation these authors started from a 'symmetrized' ps representation of the form

$$T^{\mathrm{I}}(|\mathbf{p}|, \theta, x) = f_1^{\mathrm{I}}(|\mathbf{p}|, \theta, x)(S - \tilde{S}) + f_2^{\mathrm{I}}(|\mathbf{p}|, \theta, x)\frac{1}{2}(T + \tilde{T})$$
$$-f_3^{\mathrm{I}}(|\mathbf{p}|, \theta, x)(A - \tilde{A}) + f_4^{\mathrm{I}}(|\mathbf{p}|, \theta, x)(V + \tilde{V}) + f_5^{\mathrm{I}}(|\mathbf{p}|, \theta, x)(P - \tilde{P})$$
(46)

for the T-matrix. Again, this ps representation is equivalent to the ps representation (17). Due to the Fierz transformation (28) the five amplitudes  $f_i^{\rm I}$  are related to the amplitudes  $F_i^{\rm I}$  by a linear transformation

$$\begin{pmatrix}
f_{1}^{I} \\
f_{2}^{I} \\
f_{3}^{I} \\
f_{4}^{I} \\
f_{5}^{I}
\end{pmatrix} = \frac{1}{4} \begin{pmatrix}
2 - 4 - 12 & 0 & 0 \\
1 & 0 & 4 & 1 & 0 \\
0 - 2 & 0 & 0 & -2 \\
1 & 2 & 0 & -1 & -2 \\
0 & 4 & -12 & 2 & 0
\end{pmatrix} \begin{pmatrix}
F_{S}^{I} \\
F_{V}^{I} \\
F_{T}^{I} \\
F_{P}^{I} \\
F_{A}^{I}
\end{pmatrix}.$$
(47)

The anti-symmetry relation (19) converts to the much simpler phase relation [26]

$$f_i^{\mathrm{I}}(|\mathbf{p}|, \pi - \theta, x) = (-)^{\mathrm{I+i}} f_i^{\mathrm{I}}(|\mathbf{p}|, \theta, x) \quad , \tag{48}$$

where i runs from 1 to 5. Applying the operator identities (45) the 'symmetrized' ps representation (46) can be rewritten as

$$T^{\mathrm{I}}(|\mathbf{p}|, \theta, x) = g_{\mathrm{S}}^{\mathrm{I}}(|\mathbf{p}|, \theta, x) \mathbf{S} - g_{\tilde{\mathbf{S}}}^{\mathrm{I}}(|\mathbf{p}|, \theta, x) \tilde{\mathbf{S}} + g_{\mathrm{A}}^{\mathrm{I}}(|\mathbf{p}|, \theta, x) (\mathbf{A} - \tilde{\mathbf{A}}) + g_{\mathrm{P}}^{\mathrm{I}}(|\mathbf{p}|, \theta, x) \mathbf{P} - g_{\tilde{\mathbf{p}}}^{\mathrm{I}}(|\mathbf{p}|, \theta, x) \tilde{\mathbf{P}} ,$$

$$(49)$$

where the new amplitudes  $g_i^{\rm I}$  are defined as

$$\begin{pmatrix}
g_{S}^{I} \\
g_{\tilde{S}}^{I} \\
g_{A}^{I} \\
g_{P}^{I} \\
g_{\tilde{P}}^{I}
\end{pmatrix} = \begin{pmatrix}
1 & 1 & 0 & 1 & 0 \\
1 & -1 & 0 & -1 & 0 \\
0 & 0 & -1 & 0 & 0 \\
0 & 1 & 0 & -1 & 1 \\
0 & -1 & 0 & 1 & 1
\end{pmatrix} \begin{pmatrix}
f_{1}^{I} \\
f_{2}^{I} \\
f_{3}^{I} \\
f_{4}^{I} \\
f_{5}^{I}
\end{pmatrix}.$$
(50)

The relation between the amplitudes  $g_i^{\text{I}}$  and  $F_i^{\text{I}}$  is given by the matrix product of the linear transformations (47) and (50), i.e.

$$\begin{pmatrix}
g_{S}^{I} \\
g_{\tilde{S}}^{I} \\
g_{A}^{I} \\
g_{P}^{I} \\
g_{\tilde{P}}^{I}
\end{pmatrix} = \frac{1}{4} \begin{pmatrix}
4 - 2 - 8 & 0 - 2 \\
0 - 6 - 16 & 0 & 2 \\
0 - 2 & 0 & 0 - 2 \\
0 & 2 - 8 & 4 & 2 \\
0 & 6 & -16 & 0 - 2
\end{pmatrix} \begin{pmatrix}
F_{S}^{I} \\
F_{V}^{I} \\
F_{T}^{I} \\
F_{P}^{I} \\
F_{A}^{I}
\end{pmatrix}.$$
(51)

Due to the linear relations between the amplitudes  $F_i^{\text{I}}$ ,  $f_i^{\text{I}}$  and  $g_i^{\text{I}}$ , all three ps representations (17), (46) and (49) of the T-matrix lead to identical results for

the nucleon self-energy. Using the representation (49) the self-energy integral reads simply

$$\Sigma_{\alpha\beta}(k, k_{\rm F}) = \int \frac{d^3\mathbf{q}}{(2\pi)^3} \frac{\theta(k_{\rm F} - |\mathbf{q}|)}{4\tilde{E}^*(\mathbf{q})} \left[ \tilde{m}_F^* \mathbf{1}_{\alpha\beta} \left( 4g_{\rm S} - g_{\tilde{\rm S}} + 4g_{\rm A} - g_{\tilde{\rm P}} \right) + \tilde{g}_{\alpha\beta}^* \left( -g_{\tilde{\rm S}} + 2g_{\rm A} + g_{\tilde{\rm P}} \right) \right] , \qquad (52)$$

where again  $g_i$  denote isospin averaged amplitudes, evaluated at relative momenta  $|\mathbf{p}|$  and scattering angle  $\theta = 0$  in the c.m. frame.

If we replace in (49) the covariants P,  $\tilde{P}$  by the pseudo-vector covariants PV,  $\tilde{PV}$ , respectively, we arrive at the 'complete' pv representation [26]

$$T^{\mathrm{I}}(|\mathbf{p}|, \theta, x) = g_{\mathrm{S}}^{\mathrm{I}}(|\mathbf{p}|, \theta, x) S - g_{\tilde{\mathrm{S}}}^{\mathrm{I}}(|\mathbf{p}|, \theta, x) \tilde{S} + g_{\mathrm{A}}^{\mathrm{I}}(|\mathbf{p}|, \theta, x) (A - \tilde{A}) + g_{\mathrm{PV}}^{\mathrm{I}}(|\mathbf{p}|, \theta, x) PV - g_{\widetilde{\mathrm{PV}}}^{\mathrm{I}}(|\mathbf{p}|, \theta, x) \widetilde{PV} ,$$
(53)

with  $g_{\text{PV}}^{\text{I}}(\theta)$  and  $g_{\widetilde{\text{PV}}}^{\text{I}}(\theta)$  being identical to  $g_{\text{P}}^{\text{I}}(\theta)$  and  $g_{\widetilde{\text{P}}}^{\text{I}}(\theta)$ , respectively. As shown in Ref. [5], this representation is able to reproduce the Hartree-Fock results for the nucleon self-energy when we use the pseudo-vector pion exchange potential as bare nucleon-nucleon interaction. The self-energy integral using this 'complete' pv representation of the T-matrix is given by

$$\Sigma_{\alpha\beta}(k, k_{\rm F}) = \int \frac{d^{3}\mathbf{q}}{(2\pi)^{3}} \frac{\Theta(k_{F} - |\mathbf{q}|)}{4\tilde{E}^{*}(\mathbf{q})} \left\{ (\tilde{k}_{\alpha\beta}^{*} - \tilde{\mathcal{I}}_{\alpha\beta}^{*}) \frac{2\tilde{q}_{\mu}^{*}(\tilde{k}^{*\mu} - \tilde{q}^{*\mu})}{4\tilde{m}_{F}^{*2}} g_{\widetilde{\rm PV}} \right. \\
+ \tilde{m}_{F}^{*} 1_{\alpha\beta} \left[ 4g_{\rm S} - g_{\tilde{\rm S}} + 4g_{\rm A} - \frac{(\tilde{k}^{*\mu} - \tilde{q}^{*\mu})^{2}}{4\tilde{m}_{F}^{*2}} g_{\widetilde{\rm PV}} \right] \\
+ \tilde{\mathcal{I}}_{\alpha\beta}^{*} \left[ -g_{\tilde{\rm S}} + 2g_{\rm A} - \frac{(\tilde{k}^{*\mu} - \tilde{q}^{*\mu})^{2}}{4\tilde{m}_{F}^{*2}} g_{\widetilde{\rm PV}} \right] \right\} . (54)$$

In Fig. 5 we show the non-selfconsistent Hartree-Fock nucleon self-energy components in nuclear matter using only the pion exchange potential as bare interaction between the nucleons. In the upper panel the ps representation as well as the 'conventional' pv representation are used while the lower panel shows the results with the 'complete' pv representation of the interaction. With the ps representation and the 'complete' pv representation one can reproduce the analytical results for the Hartree-Fock nucleon self-energies if we use either the pseudo-scalar or the pseudo-vector  $\pi NN$  vertex for the pion exchange potential, respectively. Hence, the 'complete' pv representation is the correct pseudo-vector representation for the interaction. On the other hand the 'conventional' pv representation leads to wrong results for the HF nucleon self-energy. In this representation the pion is not completely treated as pseudo-vector. Fig. 5 also shows the influence of the single-pion exchange potential

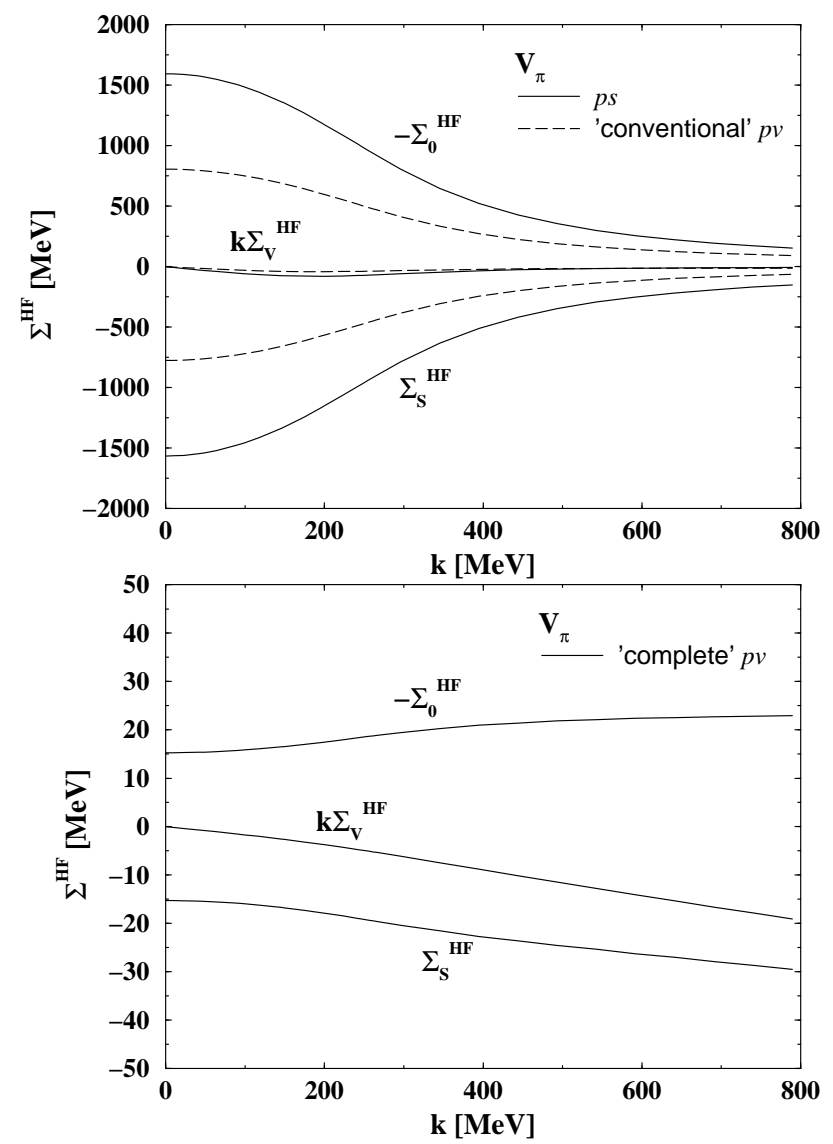


Fig. 5. Momentum dependence of the non-selfconsistent Hartree-Fock nucleon self-energy components in nuclear matter at  $k_{\rm F}=1.34fm^{-1}$ . As bare nucleon-nucleon interaction the single-pion exchange potential is used. In the upper panel the ps representation (Eq. (17, solid) and the 'conventional' pv representation (see text after Eq. (43), dashed) of the interaction are used. The lower panel shows the result using the 'complete' pv representation (Eq. (53), solid) of the interaction.

to the nucleon self-energy. Only when we use the 'complete' pv representation the contribution of the pion to the nucleon self-energy is weak. In all other cases, pseudo-scalar or 'conventional' pseudo-vector, the influence of the pion is extremely strong, i.e. the contribution to the self-energy is at least one or two orders of magnitude larger than in the complete pseudo-vector case.

In Fig. 6 we present the full self-consistent DBHF calculation with the 'compete' pv representation of the T-matrix [5]. The DBHF nucleon self-energy components are indeed weakly momentum dependent. The single-pion exchange contribution to the interaction, which was previously dominating at

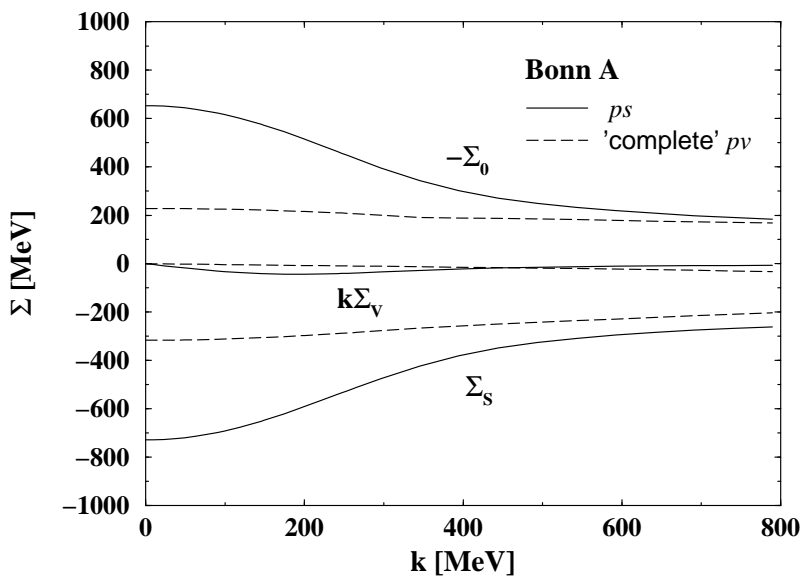


Fig. 6. Momentum dependence of the DBHF nucleon self-energy components in nuclear matter at  $k_{\rm F}=1.34fm^{-1}$  using Bonn A as bare nucleon-nucleon interaction. For the T-matrix the ps representation (Eq. (17), solid) and the 'complete' pv representation (Eq. (53), dashed) are applied.

low nucleon momenta, is now strongly suppressed. Consequently the result within the 'complete' pv representation using the Bonn A potential resembles the result within the  $\sigma$ - $\omega$  model potential, see Fig. 1 where the ps representation was used. To suppress the pion contribution to the in-medium T-matrix a correct pseudo-vector like covariant representation is essential for the calculation of the nucleon self-energy in nuclear matter. As it is necessary for the whole calculation scheme, the weak momentum dependence of the nucleon self-energy is also in accordance with the 'reference spectrum approximation' used in the calculation. The current DBHF approach therefore appears to be self-consistent.

#### 3.4 Covariant representations of the subtracted T-matrix

The 'complete' pv representation successfully reproduces the HF nucleon self-energy in the case of the pion exchange. Hence, this representation is at the moment the 'best' representation of the on-shell T-matrix which is accordance with the pseudo-vector nature of the pion exchange potential. However, as already pointed out in [5], the 'complete' pv representation fails to reproduce the HF nucleon self-energy if other meson exchange potentials are applied as bare interaction. This is demonstrated in Fig. 7 where we consider as an example the single-omega exchange. While the ps representation of the interaction correctly reproduces the analytical HF nucleon self-energy, the 'complete' pv representation fails in this respect. In particular the scalar and vector self-energies are shifted by about 200 MeV. The failure of the 'complete' pv

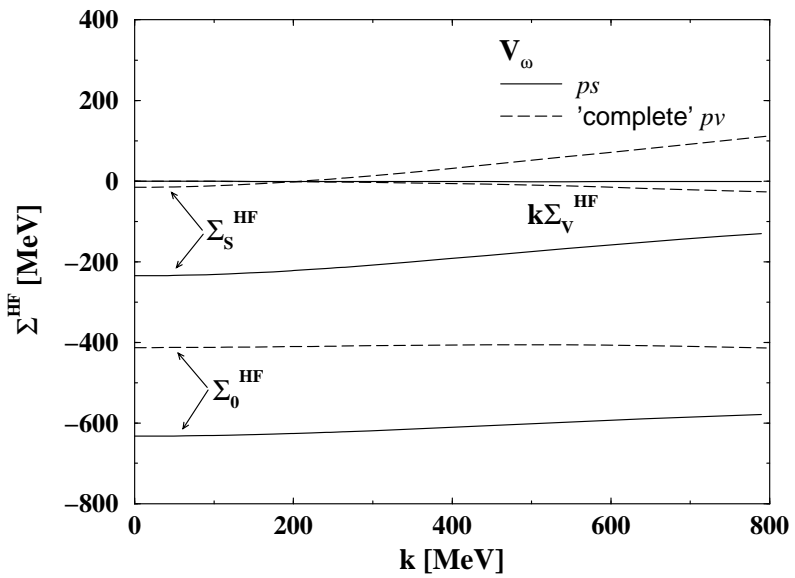


Fig. 7. Momentum dependence of the non-selfconsistent Hartree-Fock nucleon self-energy components in nuclear matter at  $k_{\rm F} = 1.34 fm^{-1}$  using as bare interaction the omega exchange potential. For the potential the ps representation (Eq. (17), solid) and the 'complete' pv representation (Eq. (53), dashed) are used.

representation is understandable since the vector covariant V in the ps representation is partially replaced by a pseudo-vector covariant when we use the identity (45) with P and  $\tilde{P}$  replaced by PV and  $\tilde{P}$ V, respectively. Since the 'complete' pv representation is not the correct covariant representation of the bare interaction, we therefore can not expect that it is correct on the level of the full in-medium interaction.

However, in the last section we have seen that the influence of the pion is dominantly given by the single-pion exchange. Hence, it should be reasonable to treat the bare interaction and the higher order ladder graphs of the meson exchange potential separately. Since the single-meson exchange potential is actually known analytically we can represent it covariantly by a mixed representation of the form

$$V = V_{\pi,\eta}^{PV} + V_{\sigma,\omega,\rho,\delta}^{P} \quad . \tag{55}$$

Here the  $\pi$ - and  $\eta$ -meson contributions are treated as pseudo-vector (49) while for the  $(\sigma, \omega, \rho, \delta)$ -meson contributions of the Bonn potential the ps representation (46) is applied. The higher order ladder diagrams of the T-matrix

$$T_{Sub} = T - V = i \int VQGGT = \sum_{n=1}^{\infty} \int V(iQGGV)^n \quad , \tag{56}$$

in the following called the subtracted T-matrix, can not be represented correctly in a mixed form since we can not disentangle the different meson con-

tributions to this part of the full in-medium interaction. The representation of the subtracted T-matrix remains therefore ambiguous. However, if the pion exchange dominantly contributes to the Hartree-Fock level a ps representation of the subtracted T-matrix should be more appropriate because then the higher order contributions of other meson exchange potentials are not treated incorrectly as pseudo-vector. Thus the most favorable representation of the T-matrix is given by the ps representation

$$T^{\mathcal{P}} = T_{Sub}^{\mathcal{P}} + V_{\pi,\eta}^{PV} + V_{\sigma,\omega,\rho,\delta}^{P} \quad . \tag{57}$$

Here the ps representation for  $T_{Sub}^{P}$  is determined via the matrix elements

$$<\mathbf{p}\lambda_{1}'\lambda_{2}'|T_{Sub}^{\mathrm{I}}(x)|\mathbf{q}\lambda_{1}\lambda_{2}>:=<\mathbf{p}\lambda_{1}'\lambda_{2}'|T^{\mathrm{I}}(x)-V^{\mathrm{I}}(x)|\mathbf{q}\lambda_{1}\lambda_{2}>$$
, (58)

with subsequently applying the projection scheme as in Eq. (??). An alternative representation of the T-matrix is given by the pv representation

$$T^{\text{PV}} = T_{Sub}^{\text{PV}} + V_{\pi,n}^{PV} + V_{\sigma,\omega,\rho,\delta}^{P} \quad , \tag{59}$$

where the subtracted T-matrix is represented by the 'complete' pv representation (53). This representation is similar to the 'complete' pv representation of the full T-matrix, however, with the advantage that now the pseudo-scalar contributions in the bare nucleon-nucleon interaction, e.g. the single-omega exchange potential, are represented correctly. In the next section we will use both representations, (57) and (59), to study the properties of nuclear matter in the DBHF approach. In this way we can determine the influence of the higher order ladder graphs to the in-medium interaction in a more quantitative way. Furthermore, these two representations set the range of the remaining ambiguity concerning the representation of the T-matrix, i.e. after separating the leading order contributions.

#### 4 Results for nuclear matter

In this section we will present results for the properties of nuclear matter using the new approach to the DBHF problem outlined in the previous section. As bare nucleon-nucleon potential we employ the one-boson exchange potentials Bonn A, B and C [12]. These potentials are based on the exchange of six non-strange bosons  $(\pi, \eta, \rho, \omega, \delta, \sigma)$  with masses below 1 GeV. For the pion and the eta meson the derivative pseudo-vector coupling is applied. The three parameterizations A,B and C of the Bonn potential differ essentially in the  $\pi$ NN form factor and, as a consequence, in the strength of the nuclear tensor force.

# 4.1 The nucleon self-energy

## 4.1.1 Momentum dependence

The momentum dependence of the nucleon self-energy at saturation density in isospin saturated nuclear matter is shown in Fig. 8. For both T-matrix

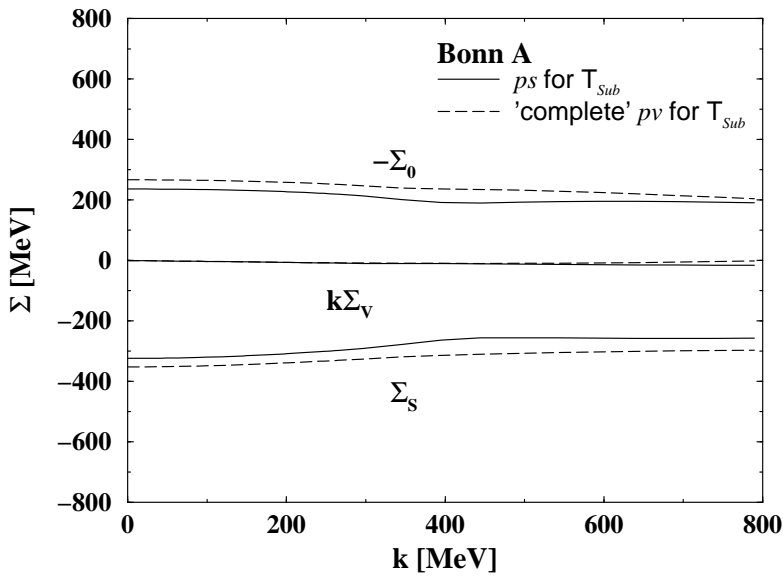


Fig. 8. Momentum dependence of the nucleon self-energy components in nuclear matter at  $k_{\rm F} = 1.34 fm^{-1}$  using Bonn A as bare nucleon-nucleon interaction. For the T-matrix the subtraction scheme with the ps representation (Eq. (57), solid) and the pv representation (Eq. (59), dashed) are applied.

representations (57) and (59), the self-energy components are rather weakly dependent on the nucleon momentum. In addition, they are also almost identical, i.e. the difference between a pseudo-scalar or pseudo-vector representation of the higher order ladder diagrams is rather small. This demonstrates again that the pion indeed contributes mostly to the Hartree-Fock level. Hence the ambiguity of the T-matrix representation has only minor influence on the final result for the nucleon self-energy in the medium

However, at larger densities of the nuclear medium the situation changes. In Fig. 9 the momentum dependence of the self-energy components in nuclear matter at a Fermi momentum of  $k_{\rm F}=1.8fm^{-1}$  is shown. Now the two representations of the T-matrix lead to significantly different results. In addition, the momentum dependence of the nucleon self-energy components is increasing for both representations. A strong momentum dependence of the self-energies at higher densities was also observed in Ref. [2]. The question how to represent the T-matrix is now much more severe than at lower densities. However, the 'complete' pv representation of the subtracted T-matrix gives a rather unphysical asymptotic behavior of the nucleon self-energy. The vector component  $\Sigma_V$ 

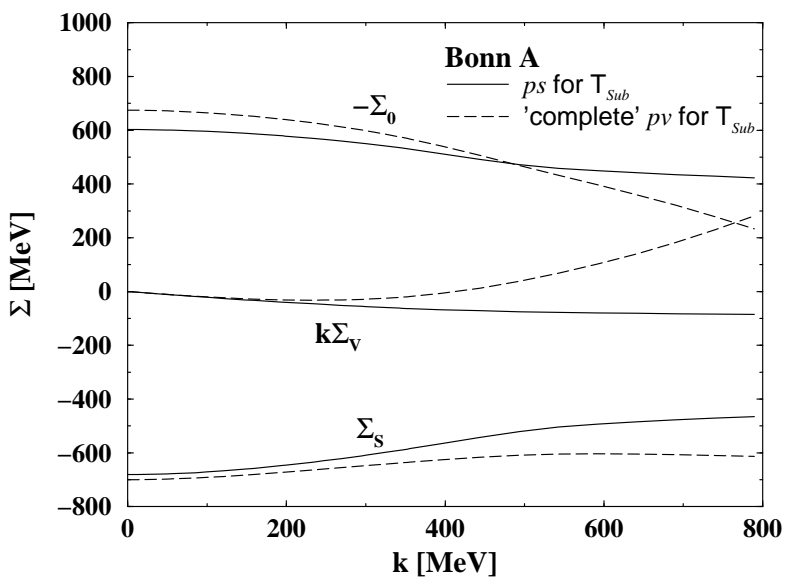


Fig. 9. Momentum dependence of the nucleon self-energy components in nuclear matter at  $k_{\rm F} = 1.8 fm^{-1}$  using Bonn A as bare nucleon-nucleon interaction. For the T-matrix the subtraction scheme with the ps representation (Eq. (57), solid) and the pv representation (Eq. (59), dashed) are applied.

not only changes sign but also increases drastically at large nucleon momenta. We believe that the misrepresentation of the higher order ladder diagrams of the heavy meson exchange potentials which should be treated as pseudo-scalar and not as pseudo-vector is responsible for this behavior. Since the *ps* representation of the ladder kernel, i.e. the subtracted T-matrix, still yields reasonable results at higher densities this representation should be preferable. Since the momentum dependence increases with increasing density, it should be included in the future in the self-consistency scheme when predictions at high densities are made [11].

In Fig. 10 we show the complete dependence of the scalar  $\Sigma_S$  self-energy and the vector component  $\Sigma_0$  on momentum and density. As bare interaction the Bonn A potential is used again while for the T-matrix the subtraction scheme with the ps representation of the ladder kernel, Eq. (57), is applied. As can be seen from Fig. 10 the momentum dependence starts to become pronounced at densities around  $\rho = 2.0\rho_0$ , where  $\rho_0 = 0.166fm^{-3}$  is the empirical saturation density of nuclear matter. At fixed density the momentum dependence is still most pronounced around the corresponding Fermi momentum. On the other hand, keeping the nucleon momentum fixed and varying the Fermi momentum, we see that the medium dependence, namely the variation of the self-energy with the nuclear matter density, is strongest for low energetic nucleons. This clearly demonstrates the influence of the Pauli-blocking effect which vanishes with increasing relative momentum of the nucleon interacting with the particles inside the Fermi sea.

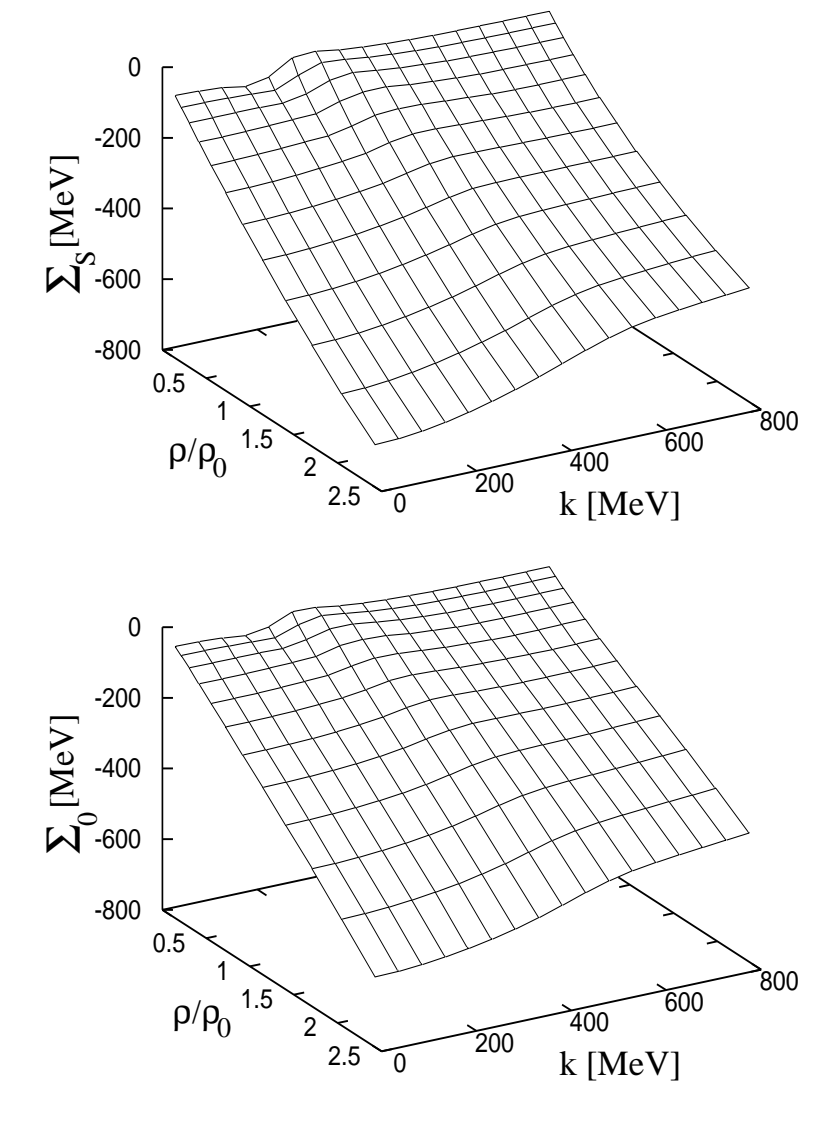


Fig. 10. Dependence of the nucleon self-energy component  $\Sigma_s$  (upper panel) and  $\Sigma_0$  (lower panel) on the nuclear matter density  $\rho$  and the nucleon momentum k. As bare interaction the Bonn A potential is used while for the T-matrix the subtraction scheme with the ps representation, Eq. (57), is applied.

# 4.1.2 Density dependence

The detailed density dependence of the nucleon self-energy components in nuclear matter is presented in Fig. 11. The momentum k of the nucleon is thereby fixed at the Fermi momentum  $k_F$ . The density dependence of the nucleon self-energy is quite similar for both representations (57) and (59) of the T-matrix. An important difference is, however, the deviation in the vector component  $\Sigma_V$ . As already seen from Fig. 9, the 'complete' pv representation of the ladder kernel leads to an unphysical behavior of the spatial  $\Sigma_V$  component.

This has a strong influence on the reduced effective mass  $\tilde{m}_F^*$  of the nucleon, Eq. (8). The reduced effective mass generally drops with increasing density

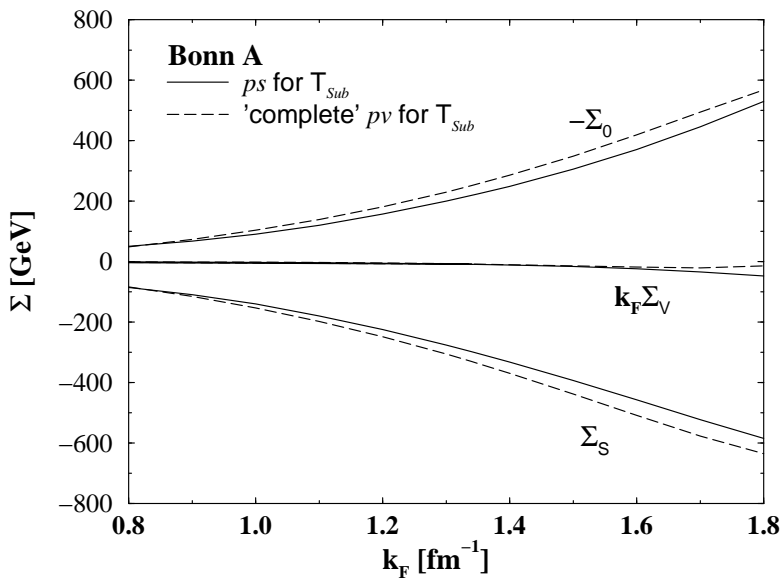


Fig. 11. Density dependence of the nucleon self-energy components in nuclear matter using Bonn A as bare nucleon-nucleon interaction. For the T-matrix the subtraction scheme with the ps representation (Eq. (57), solid) and the pv representation (Eq. (59), dashed) are applied.

as can be seen from Fig. 12 where the reduced effective mass is shown as a function of the Fermi momentum. At saturation density, for Bonn A at

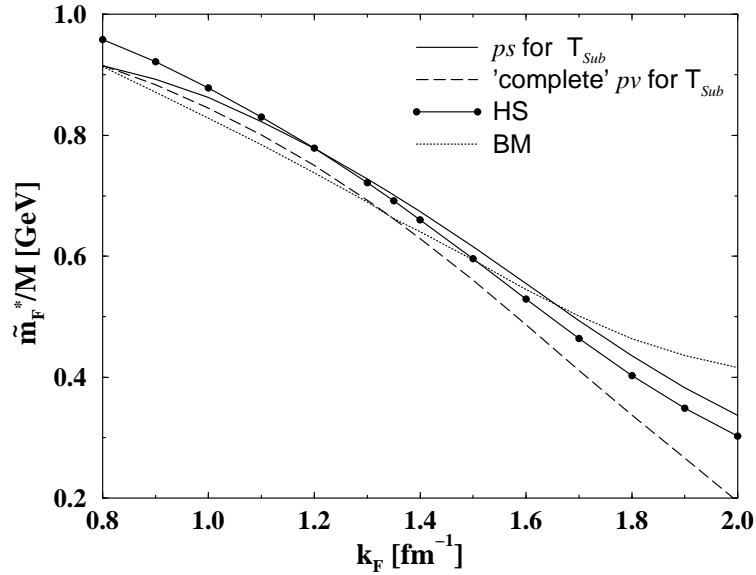


Fig. 12. Density dependence of the reduced effective mass  $\tilde{m}_F^*$  of the nucleon in nuclear matter, using Bonn A as bare nucleon-nucleon interaction. For the T-matrix the subtraction scheme with the ps representation (Eq. (57), solid) and the pv representation (Eq. (59), dashed) are applied. In addition the result of Horowitz and Serot (HS) (Ref. [1], solid with circles) and of Brockmann and Machleidt (BM) (Ref. [3], dotted) are shown.

 $k_F = 1.39 fm^{-1}$ , the reduced effective mass has a value of  $\tilde{m}_F^* \sim 0.65 M$  for both T-matrix representations. This agrees with the findings of other groups

[1,3] and also with the empirical value determined from the spin-orbit interaction in finite nuclei [30]. At larger densities, however, the two representations for the T-matrix lead to rather different results. At a Fermi momentum of  $k_F = 2.0 fm^{-1}$ , which is three times nuclear matter density, the results differ by almost a factor of two. The solid curve with circles shown in Fig. 12 is the result of the calculation by Horowitz and Serot [1], who used as bare nucleonnucleon interaction the  $\sigma$ - $\omega$  model potential. Since they did not consider the pion in their calculation they used the ps representation for the full in-medium T-matrix. Fitting the saturation properties of nuclear matter, their result for the effective mass is almost identical to our calculation with the ps representation (57) of the subtracted T-matrix. The calculation of Brockmann and Machleidt [3] is shown as dotted curve in Fig. 12. These authors used instead of the projection technique a fit procedure to the single-particle potential. They assumed a momentum independent form of the nucleon self-energy and thus they could obtain only approximately the effective mass of the nucleon. For lower densities their result is, however, quite similar to our findings. Only at higher densities important differences occur. In their calculation the effective mass seems to saturate much earlier while in our calculation with the psrepresentation of the subtracted T-matrix the effective mass drops to a smaller value at larger densities.

The above analysis indicates again that the ps representation of the remaining ladder kernel of the T-matrix is preferable compared to the 'complete' pv representation. Although the two alternatives proposed here yield similar results at densities below and up to saturation, the different representations become decisive with increasing density. The 'complete' pv representation of the ladder kernel of the T-matrix leads thereby to a partially unphysical high density behavior, i.e. a too strongly dropping mass, whereas the ps representation is still reasonable. For completeness the various relevant quantities as a function of the nuclear matter density are presented in Tab. 1 using the subtraction scheme with the ps representation (57) for the subtracted T-matrix. As bare nucleon-nucleon interaction the Bonn A potential is used.

## 4.2 The equation-of-state of nuclear matter

In the relativistic Brueckner theory the energy per particle is defined as the kinetic plus half the potential energy

$$E/A = \frac{1}{\rho} \sum_{\mathbf{k}, \lambda} \langle \bar{u}_{\lambda}(\mathbf{k}) | \boldsymbol{\gamma} \cdot \mathbf{k} + M + \frac{1}{2} \Sigma(k) | u_{\lambda}(\mathbf{k}) \rangle \frac{\tilde{m}^{*}(k)}{\tilde{E}^{*}(k)} - M \quad . \quad (60)$$

In Fig. 13 we show the binding energy per particle E/A as a function of the density, calculated with Bonn A, B and C. For the T-matrix the subtraction

Table 1 The Fermi-momentum  $k_{\rm F}$ , the nuclear matter density  $\rho$ , the binding energy per particle E/A, the reduced effective mass  $\tilde{m}_F^*$  and the components of the nucleon self-energy (at  $|\mathbf{k}| = k_{\rm F}$ ) for nuclear matter applying the ps representation (57) for the subtracted T-matrix. As bare nucleon-nucleon interaction the Bonn A potential is used.

$k_{ m F}$	ρ	E/A	$\tilde{m}_F^*$	$\Sigma_s$	$-\Sigma_0$	$\Sigma_v$
$[\mathrm{fm}^{-1}]$	$[\mathrm{fm}^{-3}]$	$[\mathrm{MeV}]$	$[\mathrm{MeV}]$	$[\mathrm{MeV}]$	$[\mathrm{MeV}]$	
0.7	0.023	-7.74	868.4	-72.0	42.1	-0.0017
0.8	0.035	-8.77	858.2	-85.6	51.1	-0.0058
0.9	0.049	-9.98	837.1	-108.8	68.0	-0.0084
1.0	0.068	-11.62	809.1	-139.5	90.6	-0.0121
1.1	0.090	-13.45	771.6	-179.2	120.9	-0.0155
1.2	0.117	-14.80	729.9	-224.0	157.3	-0.0207
1.3	0.148	-15.74	682.8	-275.2	200.3	-0.0281
1.35	0.166	-16.03	657.8	-303.0	224.2	-0.0333
1.4	0.185	-16.15	632.1	-331.8	249.5	-0.0395
1.5	0.228	-15.28	577.8	-392.6	305.8	-0.0546
1.6	0.277	-12.37	520.4	-457.0	371.1	-0.0741
1.7	0.332	-6.19	462.9	-522.2	445.8	-0.0999
1.8	0.394	4.78	408.4	-584.6	530.2	-0.1325
1.9	0.463	22.22	358.9	-641.4	626.4	-0.1712
2.0	0.540	48.19	315.9	-690.8	735.6	-0.2146

scheme with the ps representation (57) is applied. With Bonn A one can reproduce the empirical saturation point of nuclear matter, shown as shaded region in the figure. The other Bonn potentials give less binding energy although the saturation density is always close to the empirically known value.

The result for the binding energy per particle using the two representations (57) and (59) for the T-matrix are very similar as can be seen in Fig. 14. At saturation density the binding energy is only 0.5 MeV smaller using the pseudo-vector representation of the subtracted T-matrix. Thus, the energy per particle is not very sensitive on the explicit representation of the subtracted T-matrix. As already noticed, on the level of the self-energies, Fig. 5, 9 and 12, differences between the two methods occur at higher densities. In particular the equation-of-state in the *ps* representation for the subtracted T-matrix

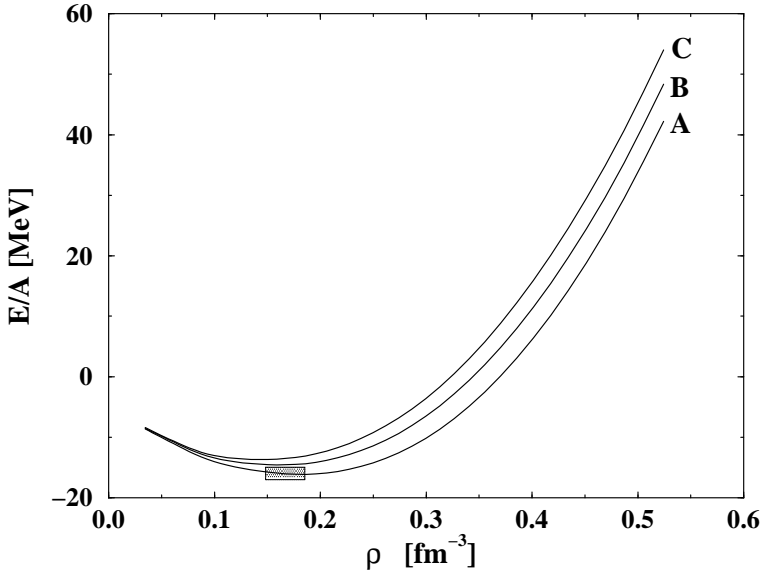


Fig. 13. Binding energy per particle as a function of nuclear matter density. As bare nucleon-nucleon interaction the potentials Bonn A, B and C are used. For the T-matrix the subtraction scheme with the ps representation (57) is applied. The shaded box denotes the empirical saturation region of nuclear matter.

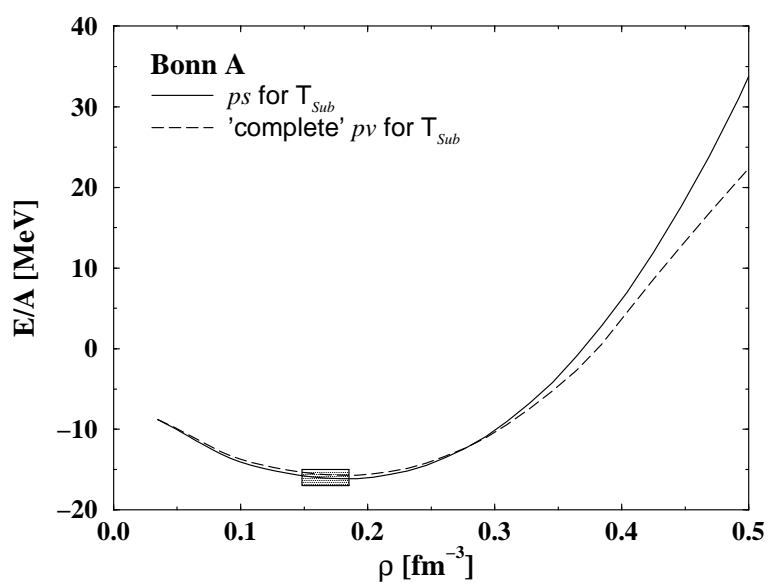


Fig. 14. Binding energy per particle as a function of nuclear matter density. As bare nucleon-nucleon interaction the Bonn A potential is used. For the T-matrix the subtraction scheme with the ps representation (Eq. (57), solid) and the pv representation (Eq. (59), dashed) are applied.

appears to be more stiff at higher densities than with the corresponding pv representation.

To understand this behavior in more detail and to compare also with other calculations we show in Fig. 15 the binding energy per particle as a function of nuclear matter density for different scenarios. First of all, applying the projec-

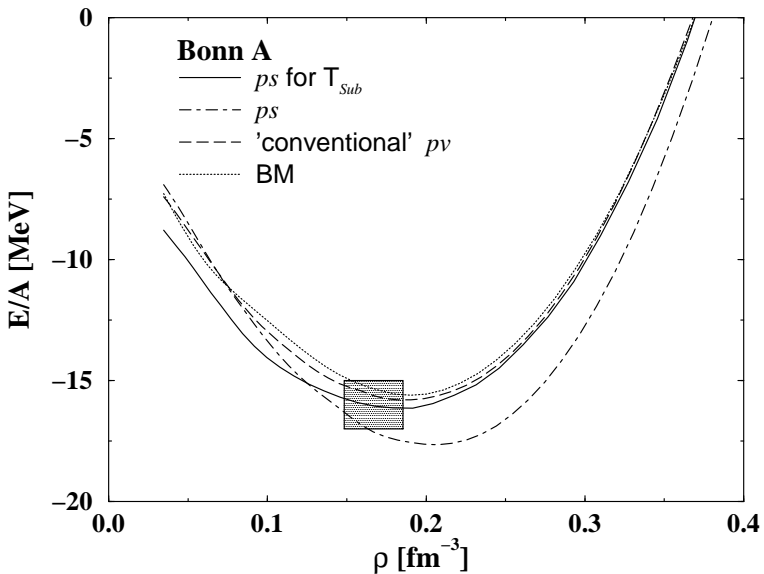


Fig. 15. Binding energy per particle as a function of nuclear matter density. As bare nucleon-nucleon interaction the Bonn A potential is used. For the T-matrix the subtraction scheme with the ps representation (Eq. (57), solid), the full ps representation (Eq. (17), dash-dotted) and the 'conventional' pv representation (see text after Eq. (43), dashed) are applied. In addition the result of Brockmann and Machleidt (BM) (Ref. [3], dotted) is shown.

tion method of Horowitz and Serot, we can reproduce almost completely the result of Brockmann and Machleidt (BM), Ref. [3], when we use the 'conventional' pv representation of the T-matrix. (see text after Eq. (43)). The two approaches are in detail compared in Tab. 3. Except of the incompressibility, which is generally smaller in our calculation, the bulk properties are indeed very similar. This result is somewhat surprising since the approach of Ref. [3] is completely different from the present one. As already mentioned, in Ref. [3] no projection scheme to the T-matrix has been applied but constant, i.e. momentum independent, self-energy components have been determined by a fit to the single particle potential. On the other hand, the 'conventional' pvrepresentation of the T-matrix leads to a pronounced momentum dependence of the self-energy components, see Fig. 4. That these two calculations give nevertheless similar results for the nuclear matter bulk properties is due to the fact that they lead to more or less identical values for the fields and the effective mass at the Fermi momentum. This agreement appears, however, to be somewhat fortuitous.

However, as discussed in the previous sections the 'conventional' pv representation does not correctly reproduce the contribution of the single-pion exchange potential to the nucleon self-energy. On the level of the binding energy one can estimate the contribution of the single-pion exchange potential comparing the result of ps representation for the subtracted T-matrix and the pure ps representation of the T-matrix. In the latter approach the nucleons are

less bound at small densities but the situation changes around saturation. A correct pseudo-vector representation of the pion, as used in the subtraction scheme, suppresses this effect. Thus at smaller densities we obtain a larger binding, while around saturation density the binding energy is smaller. Compared to the 'conventional' pv representation or the result of Brockmann and Machleidt, the ps representation of the subtracted T-matrix plus a correct treatment of the bare interaction leads altogether to more binding at smaller and medium densities. The correct treatment of the single-pion exchange potential is therefore essential in the low density regime of the equation-of-state. Except of the pure ps treatment, which is certainly not correct for a realistic potential like the Bonn potential [10,2,5], the various calculations coincide at high densities. This reflects a decreasing relative importance of the pion-exchange at high densities.

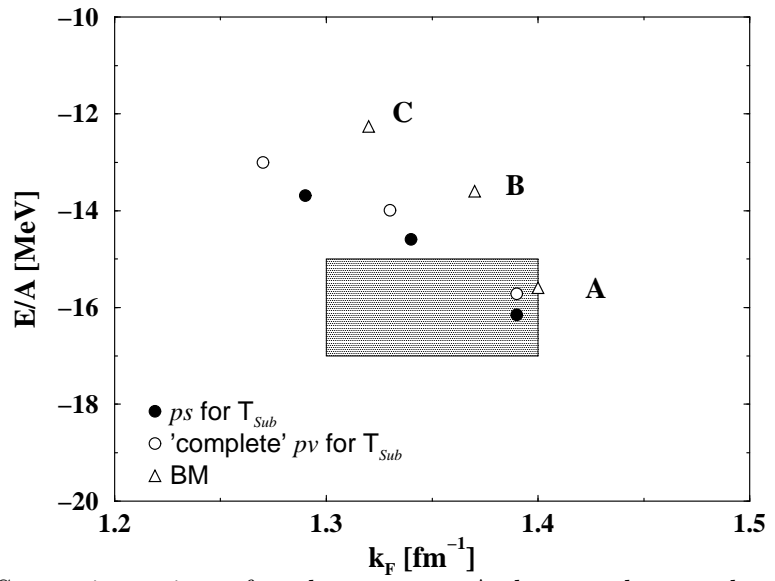


Fig. 16. Saturation points of nuclear matter. As bare nucleon-nucleon interaction the Bonn potentials A,B and C are used. For the T-matrix the subtraction scheme with the *ps* representation (Eq. (57), filled circles) and the *pv* representation (Eq. (59), open circles) are applied. As open triangles the results of the calculation of Brockmann and Machleidt (BM), Ref. [3], are shown.

The present results are summarized in Fig. 16 where the corresponding saturation points for the three different versions of the Bonn potential are shown. We compare the results with the two representation of the subtracted T-matrix with the results of the calculation of Brockmann and Machleidt (BM), Ref. [3]. With the improved representation schemes (57) and (59) for the T-matrix one obtains new 'Coester-lines' which are left of the original one, i.e. shifted towards the empirical region. The refined treatment of the T-matrix representation leads to an enhancement of the binding energy connected with a reduced saturation density. As in the previous calculations, Bonn A is still the only one which meets the empirical region. However, due to an increased binding energy Bonn B is now much closer to empirical region. This observation

is consistent with the present treatment. The different types of Bonn potentials essentially vary in the strength of the nuclear tensor force determined by the  $\pi NN$  form factor. Bonn A which has the smallest tensor force yields the smallest D-state probability of the deuteron and only a pure description of the  $^3D_1$  phase shift [3,12]. Thus it appears that a refined treatment of the pion exchange leads to improved nuclear matter results for the more realistic Bonn B potential. Bonn C, however, is still far off the empirical region.

Furthermore, it can be seen from Fig. 16 and Tab. 2 that the final nuclear matter bulk properties depend only moderate on the representation of the subtracted T-matrix. In Ref. [5] we tried already to determine the range of inherent uncertainty in the relativistic Brueckner approach which is due to the ambiguities concerning the representation of the T-matrix discussed in Section 3. By the separate treatment of the Born contribution to the T-matrix we end up now with a much narrower uncertainty band which is given by the ps or complete pv representation of the ladder kernel, i.e. the subtracted Tmatrix. Over the different types of Bonn interactions the two methods lead to a variation of 0.5 MeV in the binding energy, 0.1–0.2  $fm^{-1}$  in the Fermi momentum, and to about 30 MeV concerning the value of the effective mass at saturation density. The values for incompressibility are also close in the two approaches, i.e. they differ by less than 10 MeV. However, compared to the conventional pv representation and especially to Ref. [3], see Tab. 3, the kompression moduli are significantly reduced for all three types of interactions when we use the new approach to the T-matrix representation, see Tab. 2. Within the ps representation of the subtracted T-matrix, Bonn B and C now yield very small kompression moduli around K = 150 MeV and K = 115 MeV, respectively. For Bonn A a value of K = 230 MeV is obtained. This value agrees with the empirical value of the kompression modulus of  $K=210\pm$ 30MeV [31]. Here Brockmann and Machleidt found much larger values for all three Bonn potentials.

Table 2 The Fermi-momentum  $k_{\rm F}$ , the binding energy per particle E/A, the reduced effective mass  $\tilde{m}_F^*$  and the kompression modulus K at saturation for nuclear matter using as bare nucleon-nucleon interaction the Bonn potentials A, B and C. For the T-matrix the subtraction scheme with the ps representation (57) and the pv representation (59) are applied.

	$ps$ for $T_{Sub}$				'complete' $pv$ for $\mathcal{T}_{Sub}$				
	$k_{ m F}$	E/A	$ ilde{m}_F^*$	K		$k_{ m F}$	E/A	$\tilde{m}_F^*$	K
	$[\mathrm{fm}^{-1}]$	$[\mathrm{MeV}]$	$[\mathrm{MeV}]$	$[\mathrm{MeV}]$		$[\mathrm{fm}^{-1}]$	$[\mathrm{MeV}]$	$[\mathrm{MeV}]$	[MeV]
A	1.39	-16.15	637.0	230		1.39	-15.72	596.0	220
В	1.34	-14.59	667.0	150		1.33	-13.99	634.0	140
С	1.29	-13.69	694.0	110		1.27	-13.00	669.0	100

Table 3 The Fermi-momentum  $k_{\rm F}$ , the binding energy per particle E/A, the reduced effective mass  $\tilde{m}_F^*$  and the kompression modulus K at saturation for nuclear matter using as bare nucleon-nucleon interaction the Bonn potentials A, B and C. For the T-matrix the 'conventional' pv representation, see text after Eq. (43), is applied. In addition the results of Brockmann and Machleidt (BM), Ref. [3], are presented.

	'conventional' pv			BM					
	$k_{ m F}$	E/A	$ ilde{m}_F^*$	K	-	$k_{ m F}$	E/A	$\tilde{m}_F^*$	K
	$[\mathrm{fm}^{-1}]$	$[\mathrm{MeV}]$	$[\mathrm{MeV}]$	$[\mathrm{MeV}]$		$[\mathrm{fm}^{-1}]$	$[\mathrm{MeV}]$	$[\mathrm{MeV}]$	$[\mathrm{MeV}]$
A	1.41	-15.81	538.0	275		1.40	-15.59	564.0	290
В	1.35	-13.70	565.0	195		1.37	-13.60	573.0	249
С	1.30	-12.31	585.0	155		1.32	-12.26	590.0	185

## 5 Summary

We have investigated the nuclear matter properties in the relativistic Brueckner approach. The required representation of the T-matrix by Lorentz invariant amplitudes suffers thereby from on-shell ambiguities concerning the pseudo-scalar or pseudo-vector nature of the interaction. We minimized this ambiguity by separating the leading order, i.e. the single-meson exchange, from the full T-matrix. Actually we represented the contributions stemming from the single-meson exchange by taking the pseudo-scalar and the pseudo-vector nature of the interaction into account. Up to now, this approach is the only one which reproduces the correct results for the T-matrix on the Hartree-Fock level. The remaining higher order correlations, i.e. the ladder kernel, are then represented either completely as pseudo-scalar or as pseudo-vector.

This method takes at best the pion contribution to the nucleon self-energy into account which, on the other hand, essentially determines the momentum dependence of the self-energy. Treating the one-pion exchange with a pseudo-vector coupling the momentum dependence is strongly suppressed as it is desired from meson phenomenology. This also favors the 'reference spectrum approximation' which was a first guess to the momentum dependence of the effective mass of the nucleon. Now the results of the calculation are much more consistent with the initial assumption of a weakly momentum dependent effective mass.

Furthermore, we have investigated the density dependence of the nucleon self-energy. The results for both scenarios for the T-matrix representation are quite similar up to saturation density. This holds also for the binding energy. Both representations lead to similar saturation properties of nuclear matter which indicates that the remaining ambiguity in the representation of the ladder kernel, i.e. the higher order correlations, is not too severe at moderate densities. However, the two schemes start to differ significantly at higher densities. There, the complete pv representation of the ladder kernel, i.e. the subtracted T-matrix, leads to an unphysical behavior, whereas the corresponding ps representation still leads to reasonable results. Thus it appears that the higher density correlations are best represented adopting the pseudo-scalar representation.

As a major result of our investigation we obtain new 'Coester lines' for the various Bonn potentials. Compared to previous treatments these are shifted towards the empirically know saturation point. Bonn A is still the only potential which really meets the empirical region of saturation, but, with improved saturation properties compared to previous treatments. The refined treatment of the pion exchange leads on the other hand also to improved results for the – from the view of the phase shift analysis – more realistic Bonn B potential.

Furthermore, we found that the equation-of-state is strongly softened compared to previous calculations. Actually with Bonn A we obtain a kompression modulus of  $K \sim 230 MeV$  which is in good agreement with the empirical value.

To summarize our results, we obtained new results for the nuclear matter properties within the projection technique employing an new method for the T-matrix representation. The final results are at lower densities almost insensitive on the explicit choice made for the representation. However, at higher densities, certain differences occur when using different representation schemes. We want to stress that the ambiguity in the projection technique is still not fully resolved yet. We plan to look on off-shell T-matrix elements in the future since off-shell matrix elements of the pseudo-scalar and pseudo-vector covariants differ significantly. We hope that this might bring more insight on what is the correct on-shell representation of the T-matrix.

## Acknowledgements

The authors would like to thank H. Müther and E. Schiller for valuable discussions.

#### References

- [1] C.J. Horowitz and B.D. Serot, Nucl. Phys. A464 (1987) 613.
- [2] B. ter Haar and R. Malfliet, Phys. Rep. 149 (1987) 207.
- [3] R. Brockmann, R. Machleidt, Phys. Rev. C42 (1990) 1965.
- [4] L. Sehn, C. Fuchs and A. Faessler, Phys. Rev. C56 (1997) 216.
- [5] C. Fuchs, T. Waindzoch, A. Faessler and D.S. Kosov, Phys. Rev. C58 (1998) 2022.
- [6] F. de Jong, H. Lenske, Phys. Rev. C58 (1998) 890.
- [7] F. Coester, S. Cohen, B.D. Day and C.M. Vincent, Phys. Rev. C1 (1970) 769.
- [8] K. Erkelenz, Phys. Rep. C13 (1974) 191.
- [9] K. Holinde, Phys. Rep. C68 (1981) 121.
- [10] C. Nuppenau, Y.J. Lee and A.D. MacKellar, Nucl. Phys. A504 (1989) 839.
- [11] C.-H. Lee, T.S. Kuo, G.Q. Li and G.E. Brown, Phys. Lett. B412 (1997) 235.

- [12] R. Machleidt, Advances in Nuclear Physics, 19, 189, eds. J.W. Negele, E. Vogt (Plenum, N.Y., 1986).
- [13] J.A. Tjon and S.J. Wallace, Phys. Rev. C32 (1985) 1667.
- [14] S. Weinberg, Phys. Rev. Lett. 116 (1968) 1568.
- [15] B. ter Haar and R. Malfliet, Phys. Rev. 36 (1987) 1611.
- [16] R. Fritz and H. Müther, Phys. Rev. 49 (1994) 633.
- [17] G.E. Brown and A.D. Jackson, The Nucleon-Nucleon Interaction (North Holland, Amsterdam, 1976).
- [18] R.H. Thompson, Phys. Rev. D1 (1970) 110.
- [19] B.D. Serot and J.D. Walecka, Advances in Nuclear Physics, 16, 1, eds. J.W. Negele, E. Vogt (Plenum, N.Y., 1986).
- [20] H.A. Bethe, B.H. Brandow and A.G. Petschek, Phys. Rev. 129 (1963) 225.
- [21] M.R. Anastasio, L.S. Celenza, W.S. Pong and C.M. Shakin, Phys. Rep. 100 (1983) 327.
- [22] P. Poschenrieder, M.K. Weigel, Phys. Rev. C38 (1988) 471.
- [23] L. Sehn, A. Faessler and C. Fuchs, J. Phys. G.: Nucl. Part. Phys. 24 (1998) 135.
- [24] M.I. Haftel and F. Tabakin, Nucl. Phys. A158 (1970) 1.
- [25] M. Rose, Elementary Theory of Angular Momentum (Wiley, N.Y., 1957).
- [26] J.A. Tjon and S.J. Wallace, Phys. Rev. C32 (1985) 267.
- [27] S. Kondratyuk and O. Scholten, nucl-th/9807077.
- [28] H.F. Boersma and R. Malfliet, Phys. Rev. C49 (1994) 233.
- [29] J.D. Walecka, Ann. Phys. (N.Y.) 83 (1974) 497.
- [30] P. Ring, Prof. Part. Nucl. Phys. 37 (1996) 137.
- [31] J.P. Blaizot, Phys. Rep. 65 (1980) 171.